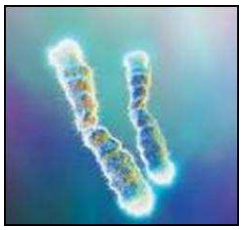

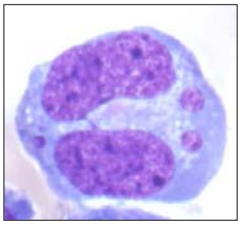

The impact of folate on telomere length and chromosome stability in human WIL2-NS cells and lymphocytes

Caroline Felicity Bull

November 2009

THE UNIVERSITY OF ADELAIDE
AUSTRALIA

SUB CRUCE LUMEN

CSIRO

CHAPTER 5:
THE EFFECT OF DNA METHYLTRANSFERASE INHIBITION BY 5-AZA-2'-DEOXYCYTIDINE ON TELOMERE LENGTH AND CHROMOSOMAL DAMAGE IN WIL2-NS CELLS *IN VITRO*

5 THE EFFECT OF DNA METHYLTRANSFERASE INHIBITION BY 5-AZA-2'-DEOXYCYTIDINE ON TELOMERE LENGTH AND CHROMOSOMAL DAMAGE IN WIL2-NS CELLS *IN VITRO*

5.1 INTRODUCTION

5.1.1 Epigenetics

The aim of the work described in this chapter was to address the possibility that hypomethylation of DNA might be a cause of increased telomere length and chromosomal instability in WIL2-NS cells. Epigenetics refers to a group of biochemical modifications to DNA and/or DNA-associated proteins (such as histones) which impact upon gene expression while the primary DNA sequence remains unchanged[310]. Methylation of cytosine in DNA, chromatin remodelling, microRNAs and post-translational modification of histones (including acetylation, methylation, phosphorylation, poly-ADP-ribosylation, ubiquitinylation, sumoylation, carbonylation and glycosylation) are all epigenetic modifications that are acquired, and are potentially heritable as markers[310,334,335]. Aberration and dysregulation of these epigenetic modifications are strongly associated with neoplastic changes and tumorigenesis[310,334,336]. While each of these modifications could play a significant role in chromosome stability and genomic integrity, it is methylation of DNA that is the primary focus of this study. Because of its role as a principal methyl donor, folate has the potential to exert a major influence on genomic integrity via this pathway.

5.1.2 DNA methylation

Methylation is an important epigenetic modification of DNA in mammals. It involves the addition of a methyl group at carbon 5 of the pyrimidine ring in cytosine, to form 5-methylcytosine[310]. Cytosine methylation is a specific form of epigenetic modification, separate and distinct from modifications to DNA-associated proteins, such as histones. DNA methylation is a mechanism for controlling gene transcription that may have evolved to silence genes of parasitic or viral origin[310]. The majority (60-90%) of CG dinucleotides (5' – CG – 3') in mammals are methylated on the cytosine residues[334,337], a distinguishing characteristic that allows detection of the hypomethylated DNA of bacteria by Toll-like receptors[338]. Mechanistically, it has been hypothesised that promoter methylation physically inhibits the

binding of transcription machinery. However, experimental evidence has shown that methylated genes are initially transcribed, but after a few hours are packaged into a less accessible chromatin structure[339,340]. These findings suggest that while DNA methylation interferes with transcription, it's main function may be to mark DNA for entry into a transcriptionally suppressed state[336,339-341].

Unmethylated cytosines are generally located in CpG-rich promoter regions, in areas known as CpG islands[310,336]. These unmethylated islands allow active gene transcription, often of key housekeeping genes, some of which have subsidiary functions as tumour suppressors. Dysregulation of epigenetic patterns is a frequent finding in neoplasia, with concurrent hypomethylation of the genome occurring as a whole together with hypermethylation of promoter-associated CpG islands. These changes can result in the activation of silenced (potentially oncogenic) genes, together with silencing of protective genes[336].

Methylation of cytosine in DNA is performed by DNA methyltransferase (DNMT) enzymes, which work in concert with methyl-CpG binding proteins (MBPs)[148,342,343]. In humans, DNMT1 is believed to be the main enzyme responsible for copying methylation patterns to new strands during replication of DNA, due to its preference for hemi-methylated DNA substrates. DNMT3a and 3b, on the other hand, are involved in the generation of new methylation patterns[341,344]. The function of DNMT2 is not yet known, but its strong binding to DNA suggests that it may mark specific sequences in the genome for methylation[345]. DNMT3L does not appear to have methyltransferase activity but it associates with DNMT3a and 3b, possibly modulating their catalytic activity[341]. MBPs contain methyl-CpG-binding domains (MBD) and belong to a family of CpG-binding proteins (MeCP2). They bind to promoters that have been methylated by DNMTs, and act to recruit chromatin remodelling co-repressor complexes, the binding of which appears to be gene- and tumour-type specific[342]. By responding to the new pattern of methylation laid down by DNMT enzymes, MBPs may be directly responsible for the aberrant gene silencing that is observed when previously unmethylated promoter sites become hyper-methylated[342]. Evidence for the methylation-dependence of MBPs was provided by experiments in which cells were exposed to a DNMT inhibitor, 5-aza-2'-deoxycytidine, *in vitro*. This treatment resulted in hypomethylation of CpG islands, the release of MBPs, and re-expression of previously repressed genes[342]. The consequences of defects in DNMT and MBD-containing proteins suggests that both have significant roles in preventing developmental abnormalities and in tumorigenesis[342,343].

5.1.3 Aberrant DNA methylation and disease

Numerous disease states have been directly attributed to aberrant DNA methylation patterns. One example, the autoimmune disease *systemic lupus erythematosus* (SLE), involves reduced DNMT1 levels and a 15-20% reduction in global DNA methylation in $CD4^+$ T lymphocytes[310]. Resulting highly auto-reactive cells $CD4^+$ T cells have been implicated in the production of anti-DNA antibodies, which are characteristic of SLE[310]. Hypomethylation in SLE is also believed to cause reactivation of endogenous retroviruses[310].

Another disease arising from genetic defects in the DNA methylation pathway is *Immunodeficiency, centromeric instability and facial anomalies (ICF) syndrome*; an extremely rare autosomal recessive condition[310]. ICF is the only disease known to be directly associated with mutations in the genes coding a *DNMT* enzyme, with only around 50 cases having been recorded worldwide since its discovery in the early 1970s[310,346]. The primary molecular defect in ICF is a mutation of the *DNMT3b* gene, resulting in defective methylation[310,346]. The disease is characterised by severe immunodeficiency that results from an absence, or significant reduction, of at least two immunoglobulin isotypes[310]. In the majority of cases the individuals have died in infancy or childhood[346]. All cases show hypomethylation and de-condensation of pericentromeric heterochromatin in B cells, involving chromosomes 1 and 16, and to a lesser extent chromosome 9[346]. Interestingly, one study has explored the mechanisms underlying the chromosomal anomalies in ICF cells and found a high degree of telomere (end-to-end) fusions between chromosomes, micronuclei containing an overrepresentation of material from chromosomes 1 and 16, and an increased frequency of anaphase (nucleoplasmic) bridges[347]. The authors concluded from these findings that associations between 1qh and 16qh at interphase had led to disturbances at mitotic segregation, formation of micronuclei, and in some cases, led to apoptosis[347].

5.1.4 Epigenetics and the telomere

Mammalian histones frequently have post-translational (epigenetic) modifications[348]. Features of telomeric heterochromatin include trimethylation of histone 3 (H3) at lysine 9 (H3K9me3) and trimethylation of histone H4 at lysine 20 (H4K20me3)[348]. These modifications are effected by "suppressor of variegation" (SUV) histone methyltransferases (HMTases)[348,349]. The role of these enzymes has been explored using a *SUV39h* double null (dn) mouse model[349]. An important observation from the dn mouse model was impaired segregation of the entire set of chromosomes, giving rise to extensive genome instability. By passage eight, the majority of primary mouse embryonic fibroblasts (PMEFs) from WT mice were senescent. In contrast, PMEFs from Suv39h dnmice continued to proliferate, displaying high levels of tetraploidy, and in some cases even octaploidy[349]. The authors concluded that Suv39h-deficient mice displayed genome instability and impaired heterochromatin, indicating the importance of histone methylation in epigenetic regulation during mammalian development[349]. This work led to the first published study linking epigenetic markers with control of telomere length with a study on the impact of homozygous inactivation of *Suv39h (Suv39h-/-* knockout) on telomere length[326]. It was found that the usual pattern of histone trimethylation at telomeric and pericentric heterochromatin in WT cells was reduced to mono- and di-methylation in the knockout cells[326]. In particular, hypomethylation of histones was shown to result in abnormally long telomeres. The authors concluded that epigenetics plays a significant role in the regulation of telomere length in mammals[326].

A further study has explored the relationship between methylation of cytosines within DNA and control of telomere length[328]. Mammalian telomeres lack CpG sequences, the substrate for DNMT, and as a result are not methylated. However, subtelomeric DNA was found to be heavily methylated[328]. Using mouse embryonic stem (ES) cells deficient either for *DNMT1*, or both *DNMT3a* and *3b*, Gonzalo *et al* (2006) demonstrated that DNA methylation of the subtelomere was significantly reduced in the absence of DNMTs while other heterochromatic marks, such as histone trimethylation, remained unaffected[328]. Most significantly, however, was the finding that the DNMT-deficient cells exhibited dramatically elongated telomeres[328]. An accompanying increase in sister chromatid exchange (SCE), involving telomeric sequences, suggested that the increase in telomere content was most likely caused by recombination. The authors cautioned, however, that they had not examined telomerase activity and dysregulation of telomere capping, leaving open the possibility that other mechanisms might be responsible[328]. Interestingly, chromosomal end-to-end fusions were not evident in this system, suggesting maintenance of the functionality of the elongated telomeres[328].

Benetti *et al* furthered discussion in this area by showing that the relationship between epigenetic markers and telomere length control may not be unidirectional[327]. Using telomerase deficient (*Terc*-/-) mouse embryonic fibroblasts (MEF), these authors demonstrated that telomere shortening correlated with a reduction in DNA methylation at the subtelomere[327]. Shortened telomeres were also associated with decreased trimethylation of histones in telomeric and subtelomeric chromatin. Together, these findings indicate that loss of telomeric repeats leads to a change in architecture of these critical regions, resulting in a more 'open' chromatin state[327]. The authors speculated that changes in telomeric and subtelomeric epigenetic modifications could provide a mechanism by which mammalian telomere repeats are counted and auto-regulated within the cell[327].

These recent reports, which demonstrate that alterations to DNA methylation can impact on control of telomere length, led to the hypothesis that hypomethylation as a result of FA deficiency could be responsible for the telomere elongation observed in WIL2-NS cells during short term FA deprivation, as presented in Chapter 4. As discussed previously, the folate pathway has two separate and distinct outcomes: (a) maintenance of cytosine methylation in DNA; and (b) methylation of dUMP to produce dTTP for incorporation of thymidine into newly synthesised DNA. Methylation of DNA is mediated by DNMT enzymes, which transfer the methyl group from S-adenosyl methionine (SAM) to DNA. This process leaves SAM in its demethylated form of S-adenosyl homocysteine, which is then converted to homocysteine (see Figure 1.4). For this cycle to continue, FA and vitamin B12 are necessary for re-methylation of homocysteine back to methionine. The previous experiments did not provide an explanation for why FA deprivation led to telomere elongation (Chapter 4). A test of the above hypothesis would be to test the effect of an agent that can induce hypomethylation. The DNMT1 inhibitor, 5-aza-2'-deoxycitidine (5azadC), was selected as a means of specifically exploring the effect of DNA hypomethylation, without the concomitant incorporation of uracil into DNA that accompanies FA deprivation.

5.1.5 5-aza-2'-deoxycytidine (5azadC)

5azadC, also known as Decitabine or Dacogen, was first synthesised in 1964[350], and was approved for the treatment of all subtypes of myelodysplastic syndrome (MDS) by the US Food and Drug Administration in 2004[351]. 5azadC is an analogue of the pyrimidine nucleoside cytidine, where the carbon at position 5 is replaced with nitrogen[350] (Figure 5.1). 5azadC, and similar synthetic compounds, are used experimentally and therapeutically to reactivate genes that may have been silenced as a result of aberrant hypermethylation at the CpG islands

associated with promoter regions[350,352]. The compound binds covalently with DNMT1, interfering with the cellular DNA methylation process[350,352].

5azadC has been shown to have a dual action as a therapeutic, exerting cytotoxicity due to incorporation into RNA and DNA, and hypomethylation of DNA by inhibiting methylation of cytosine. The latter is believed to restore normal growth control and differentiation in aberrantly hypermethylated haematopoietic cells[351]. The hypomethylating effect is understood to occur at lower doses than those required for the cytotoxic effects of the compound, as the concentration required for maximum inhibition of DNA methylation *in vitro* does not suppress DNA synthesis[351]. Following uptake into the cell, 5azadC is phosphorylated firstly to 5-azacytidine monophosphate, and then to a di- and tri-phosphate form. It is the latter that is incorporated into RNA, disrupting RNA metabolism and protein synthesis, while the diphosphate form can be incorporated into DNA after reduction to 5-aza-2'-deoxycytidine, followed by phosphorylation to a triphosphate form[351]. DNMT1 activity is inhibited when the enzyme becomes irreversibly bound to the altered cytosine residue in DNA[350,352]. This causes a rapid, passive loss of DNMT1 activity in the cell as increasing numbers of DNMT1 molecules become unavailable to methylate newly synthesised DNA sequences[352]. Accordingly, as a therapeutic, 5azadC is only effective when used in proliferating cells[352]. The hypomethylating effect becomes more pronounced after several cell divisions, as numbers of free DNMT1 molecules are gradually depleted[350]. Adducts created by the DNMT bound to 5azadC have been shown to be highly toxic and mutagenic, if not repaired[352], and they may induce cell death by obstructing DNA synthesis[350]. These adducts may also induce DNA damage through structural instability at the site of incorporation[350].

For the purposes of the present study, the lowest possible doses of 5azadC were used, with the intention of maximising hypomethylation of DNA, while minimising the cytotoxic and potentially damaging effects of DNMT DNA adducts.

5.1.6 Aims

1. To determine the effect of 5azadC treatment on telomere length in WIL2-NS cells cultured in FA-replete medium.
2. To determine whether the level of chromosomal instability, assessed using the CBMN Cytome assay, increases in WIL2-NS cells cultured in FA-replete medium containing 5azadC.

5.1.7 Hypotheses

1. Inhibition of DNMT by 5-aza-2'-deoxycytidine (5azadC), under FA-replete conditions, causes telomere elongation in WIL2-NS cells.
2. Reduced DNA methylation, due to DNMT inhibition, results in increased chromosomal instability (CIN) in WIL2-NS cells.

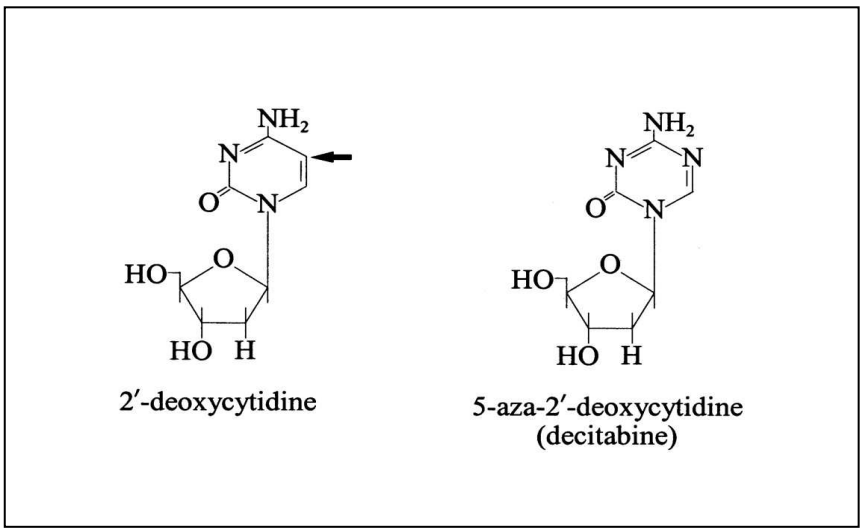

Figure 5.1 The natural nucleoside deoxycytidine, compared to the DNMT inhibitor 5-aza-2'deoxycytidine (5azadC). The arrow indicates the 5 position which is modified from a carbon in the former, to a nitrogen in 5azadC. It is this site that is the target for methylation by DNMT1. *(Adapted from Goffin & Eisenhauer, Annals of Oncology, 2002)*

5.2 EXPERIMENTAL DESIGN

WIL2-NS cells were grown in bulk cultures at different 5-aza-2'-deoxycytidine (5azadC) concentrations. The cultures were sampled at different time-points for estimation of cell numbers, cell viability and the biomarkers shown in Figure 5.2.

5mg 5azadC was obtained in powder form (Sigma, Australia) and was dissolved in 1ml PBS to form a 5mg/ml stock solution (21.9mM). This solution was sterilised by filtration and stored in aliquots for up to four weeks at -20°C. Pilot studies were conducted with WIL2-NS cells cultured in complete medium (prepared as described in Chapter 3.2.2.1) containing either 0.2, 1.0, 5.0 and 10µM 5azadC. Results of the pilot studies indicated that 0.2 and 1.0µM were optimal concentrations for maintaining a growth rate sufficient to perform experimental assays extending up to four-days. This period was chosen because previous experiments had shown that it was sufficient to produce large changes in DNA methylation, as well as the development of micronuclei[353-355].

In setting up the experiment, cells were thawed from liquid nitrogen storage, washed twice in RT PBS and grown in complete medium that was replete in FA (3000nM) for seven days. The cultures were then split (day 0 of the experiment) into three different 5azadC treatments: 0, 0.2 and 1.0µM. Cultures were maintained at 90ml total volume in a 75cm^2 vented-cap culture flask. Duplicate flasks were set up at day 0 to cater specifically for each sample day, totalling eight flasks per treatment. Each day, two flasks were removed for analysis. It was necessary to vary the initial seeding concentration of flasks, depending on the treatment condition, to achieve the required numbers of viable cells for each sample point (37 x 10^6) and to prevent overcrowding. The seeding plan was based on pilot experimentation and is detailed below at Table 5.1. Cells were sampled at day 0, 1, 2, 3 and 4 for cell numbers (Coulter Counter, Chapter 3.2.2), cell viability (Trypan blue exclusion, Chapter 3.2.3), measurement of telomere length (TL) and examination of chromosomal damage biomarkers. Total growth in each condition was calculated by counting the numbers of viable cells in the culture at the time of harvesting and extrapolating to the numbers that would have been expected if all cells had been re-seeded at each split. TL was measured by flow cytometry (n = 20 at day 0, n = 10 replicate measures per treatment per time point thereafter) (as detailed in Chapter 3.4) and chromosomal damage was assessed using the Cytokinesis Block Micronucleus Cytome (CBMN Cyt) assay (n = 2 slides were scored, a total of 1000 binucleated (BN) cells per slide per treatment per time point) (Chapter 3.3). For the CBMN Cytome assay, cells were harvested 24 hours following the addition of Cyto-B. Thus day 0 cell samples received Cyto-B at day 0, but were harvested after a further 24 hours in culture (i.e. on day 1), and so on (Figure 5.2).

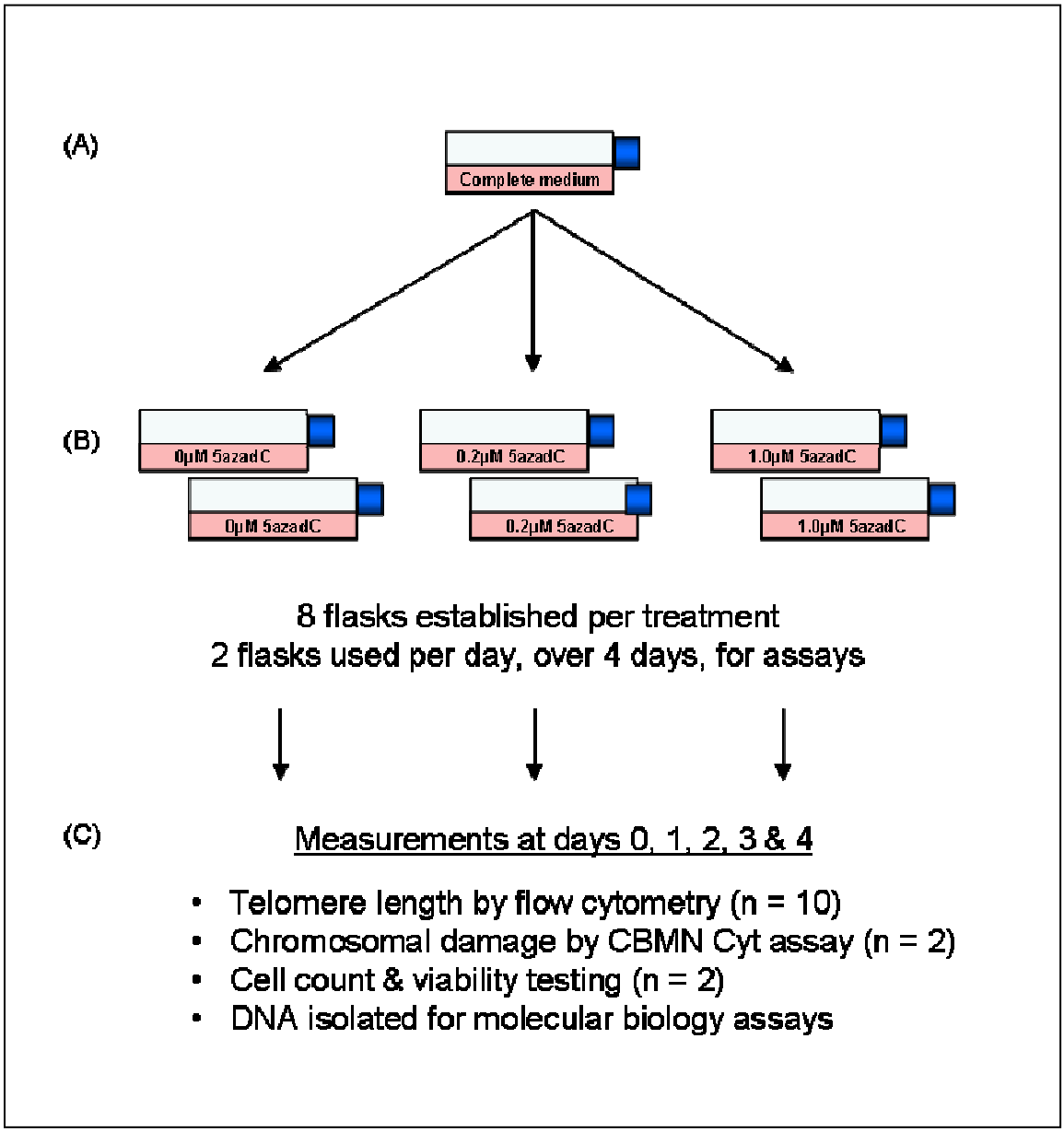

Figure 5.2 Overview of experimental design to study the response of WIL2-NS cells to culture in 5-aza-2'-deoxycytidine (5azadC). (A) Cells were thawed from liquid nitrogen storage, washed twice in PBS and cultured in FA-replete (3000nM) complete medium for 7 days prior to (B) splitting into duplicate cultures with complete medium containing either 0, 0.2 or 1.0μM 5azadC (Day 0). Each treatment was cultured in eight flasks, providing duplicate flasks for each of the four sample days. (C) Two flasks from each treatment were removed every 24 hours and assays conducted as specified.

Table 5.1 Seeding plan to study the response of WIL2-NS cells to culture in 5-aza-2'-deoxycytidine (5azadC). The cell seeding plan was based on pilot experimentation and aimed to generate the required numbers of viable cells for assays at each sample point (37 x 10^6), while preventing overcrowding. Eight flasks per treatment were seeded at day 0. Two flasks were removed per day from each treatment, the cells were harvested and aliquots were analysed for telomere length and assessed for biomarkers of chromosomal damage.

5azadC concentration	Sample day	Number of flasks	Viable cells seeded per flask at day 0 (million)	Estimated fold growth at sample day	Estimated cell number (million)	Viability (%)	Approximate viable cells (million)
0µM	1	2	15	2x	60	90	65
	2	2	5	5x	50	90	45
	3	2	2	15x	60	85	50
	4	2	1	30x	60	85	50
0.2µM	1	2	15	2x	60	90	65
	2	2	12.5	2x	50	90	45
	3	2	5	8x	80	75	60
	4	2	5	8x	80	65	52
1.0µM	1	2	15	2x	60	85	50
	2	2	15	2x	60	85	50
	3	2	10	5x	100	60	60
	4	2	10	5x	100	40	40

5.3 RESULTS

5.3.1 Cell growth, viability, nuclear division index (NDI) & necrosis

Cells cultured in medium containing 5azadC exhibited a considerably reduced growth rate, compared with controls grown in medium without 5azadC. Two-way ANOVA analysis indicated that 18.9% of growth variance was attributable to 5azadC concentration ($p < 0.0001$), while 28.8% was due to time ($p < 0.0001$). 52.3% of variance was due to the interaction of treatment with time ($p < 0.0001$) (Figure 5.3A). At days 2 and 3, Bonferroni post-test indicated significant differences in growth between the 0 and 0.2µM, and the 0 and 1.0µM conditions, while at day 4 growth differed significantly between all three treatments (Figure 5.3A).

5azadC treatment also affected the viability of WIL2-NS. There was a sharp reduction in viability, commencing between day 2 and day 3, and this effect was greatest at the highest concentration of 5azadC (1.0µM). At this concentration of 5azadC, viability was reduced from 88.6% at day 2, to 40.6% at day 4. When analysed by two-way ANOVA, approximately 19.8% of the observed variance in viability of cells grown under each condition was found to be due to 5azadC treatment ($p < 0.0001$), 59.6% to time ($p < 0.0001$) and 19.2% to the interaction of treatment with time ($p < 0.0001$) (Figure 5.3B).

The percentage of cells with morphological evidence of necrosis increased from day one in both the 0.2 and 1.0µM 5azadC treatments, with approximately 50% cell death by day four in medium containing 1.0µM 5azadC. A significant 31.9% of the variance was attributable to the treatment ($p = 0.0002$), and 39.4% to time ($p = 0.0004$), while 13.8% was due to interaction of treatment with time ($p = 0.17$) (Figure 5.3C).

Treatment with 5azadC also reduced the nuclear division index (NDI). By day four of treatment, NDI was reduced from ~1.3 in untreated cells to ~1.0 and ~0.7 in cells cultured in 0.2 and 1.0µM 5azadC respectively. Of the variance, 38.0% was due to treatment ($p < 0.0001$), 34.8% to time ($p < 0.0001$) and 19.1% to the interaction of treatment and time ($p = 0.0065$) (Figure 5.3D).

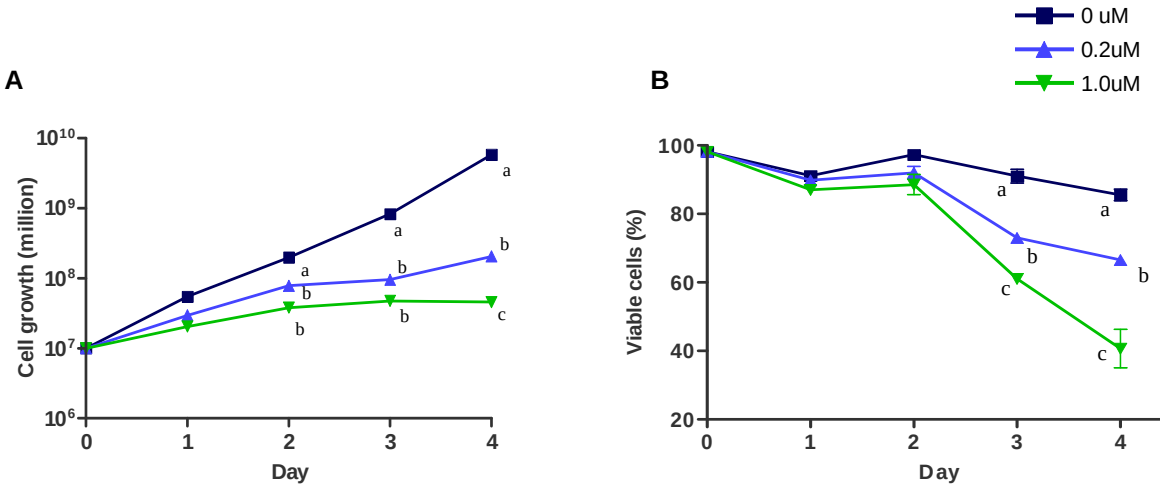

Source of variation	% of total variation	P value
Interaction	52.33	< 0.0001
5azadC	18.91	< 0.0001
Time	28.75	< 0.0001

Source of variation	% of total variation	P value
Interaction	19.16	< 0.0001
5azadC	19.76	< 0.0001
Time	59.61	< 0.0001

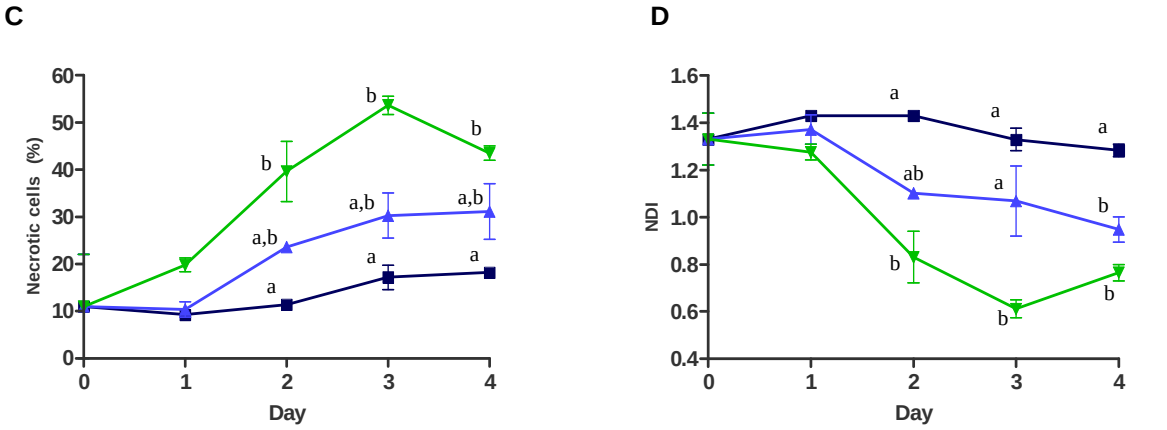

Source of variation	% of total variation	P value
Interaction	13.77	0.1714
5azadC	31.94	0.0002
Time	39.37	0.0004

Source of variation	% of total variation	P value
Interaction	19.06	0.0065
5azadC	38.04	< 0.0001
Time	34.79	< 0.0001

Figure 5.3 Effect of 5-aza-2'-deoxycytidine (5azadC) concentration on WIL2-NS cells cultured in FA-replete (3000nM) medium containing 0, 0.2 or 1.0μM 5azadC over 4 days. (A) Cell growth (calculated as described in 5.2); (B) Cell viability assessed by Trypan blue exclusion (%); (C) Cells with morphological features of necrosis (%); (D) Nuclear division index (NDI). (N = 2. Points not sharing the same letter at each time point differ significantly, as measured by the Bonferroni post test. Error bars indicate SD).

5.3.2 Assessment of telomere length by flow cytometry

Treatment with 5azadC caused a significant increase in TL, as measured by flow cytometry. In control cultures, TL remained relatively constant, with the exception of an unexplained increase at day two of culture. Relative to day 0 (19.2 ± 1.5), cells cultured in 1.0µM 5azadC exhibited a 172% increase in TL during the first 24 hours (33.1 ± 1.9), and a 156% increase relative to cells that were maintained in 0µM 5azadC for the same period (21.2 ± 1.7). At days 3 and 4, TL in cells cultured in 1.0 and 0.2µM 5azadC were ~150% and ~130% greater, respectively, than in cells cultured for the same time period without 5azadC (Figure 5.4 & Table 5.2).

Analysis by two-way ANOVA indicated 5azadC concentration was responsible for 25.3% of the variance ($p < 0.0001$), 32.7% was due to time ($p < 0.0001$), and 30% was attributable to the interaction of treatment with time ($p < 0.0001$) (Figure 5.4 & Table 5.2).

Analysis by one way ANOVA, and Tukey's post test method showed highly significant differences between TL in cells cultured in 0 or 0.2µM and those cultured in 1.0µM 5azadC at day 1 ($p < 0.0001$), between 0.2µM and either 0µM or 1.0µM at day 2 ($p < 0.0001$), and significant differences between all three conditions at days 3 and 4 (Table 5.2).

When comparisons were made of areas under the curves (AUC) for the data presented in Figure 5.4 (AUC TL), a strong positive correlation was observed between concentration of 5azadC in medium and AUC TL ($r = 0.99$), and this relationship was significant ($p < 0.0001$) (Figure 5.5).

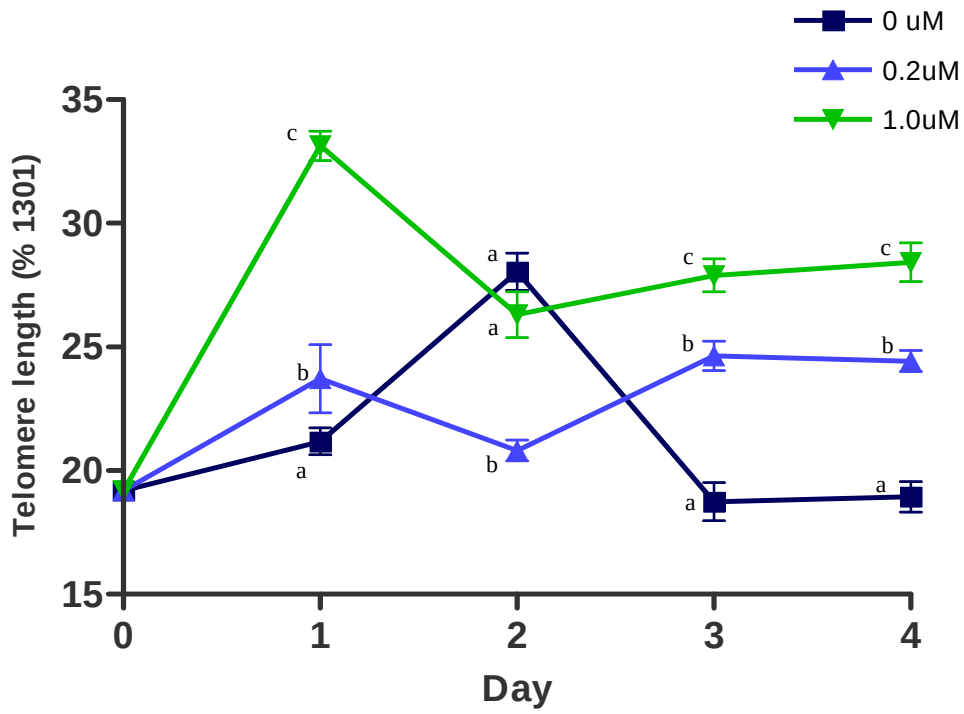

Source of variation	% of total variation	P value
Interaction	30.01	< 0.0001
5azadC	25.30	< 0.0001
Time	32.69	< 0.0001

Figure 5.4 Telomere length (TL), measured by flow cytometry, in WIL2-NS cells grown in FA-replete medium containing 0, 0.2 or 1.0μM 5-aza-2'-deoxycytidine (5azadC) over 4 days. (N = 20 at day 0, n = 10 for all times thereafter. The TL of each sample was calculated relative to the TL of the reference standard 1301 cell line. Error bars indicate SD. Points not sharing the same letter at each time point differ significantly, as measured by the Bonferroni post test. Data table represents the results of analysis by two-way ANOVA).

Table 5.2 Telomere length (TL) measured by flow cytometry. WIL2-NS cells were grown in FA-replete (3000nM) medium containing 0, 0.2 or 1.0μM 5-aza-2'-deoxycytidine (5azadC) over 4 days. (N = 20 at day 0, n = 10 at all times thereafter. Data represents mean ± SD. P values are shown for comparisons between treatments by one-way ANOVA at each time point. Data not sharing the same letter at each time point differ significantly, as measured by Tukey's post test method. Also shown is area under the curve (AUC TL) calculated for TL versus time for each treatment).

Day	*0μM*	*0.2μM*	*1.0μM*	*One-way ANOVA P value*
0	19.19 ± 1.51	19.19 ± 1.51	19.19 ± 1.51	
1	21.22 ± 1.73[a]	23.77 ± 4.35[a]	33.12 ± 1.89[b]	*< 0.0001*
2	28.04 ± 2.38[a]	20.81 ± 1.33[b]	26.31 ± 2.93[a]	*< 0.0001*
3	18.74 ± 2.42[a]	24.64 ± 1.92[b]	27.89 ± 2.1[c]	*< 0.0001*
4	18.94 ± 1.95[a]	24.43 ± 1.35[b]	28.43 ± 2.46[b]	*< 0.0001*
AUC	87.03	90.99	111.1	

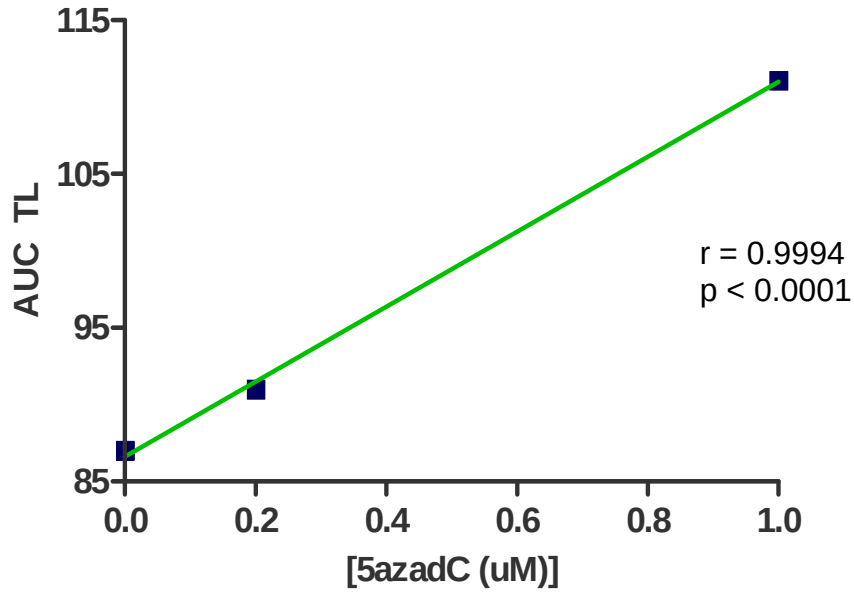

Figure 5.5 Correlation between 5azadC concentration in medium (μM) and the AUC TL for WIL2-NS cells cultured over 4 days.

5.3.3 Chromosome damage

5.3.3.1 Frequency of BN cells displaying one or more DNA damage biomarker

The results in this section, and in Table 5.3, show the frequency of BN cells that display one or more of the biomarkers of DNA damage examined in the CBMN Cyt assay (MNi, NPB, NBuds), per 1000 BN cells. Each BN cell containing a damage event, irrespective as to whether it contains one or multiple DNA damage biomarkers, is recorded as a single event in this data.

Treatment with 5azadC caused a dose-dependent increase in the frequency of BN cells displaying one or more DNA damage event for each of the biomarkers (MNi, NPB, NBuds, individually and collectively) at each time point (Table 5.3). Analysis by two-way ANOVA indicated that 5azadC concentration in medium was responsible for the significant increases observed in the frequency of BN cells displaying one or more MNi ($p < 0.0001$), one or more NPB ($p < 0.0001$) and one or more NBud ($p < 0.0001$) (Table 5.3).

The frequency of cells containing one or more MNi increased by over 600% over the 4 day study, from 17 ± 1.4 (mean ± SD) at day 0 to 103 ± 19.8 in the highest 5azadC concentration (1.0µM). Over the same time period MNi in cells in 0.2µM 5azadC increased 464% to 79.5 ± 0.7, while the frequency of MNi in cells cultured medium without 5azadC (0µM) decreased to 6.5 ± 2.1 (Table 5.3A).

BN cells displaying one or more NPB increased from 17 ± 4.2 at day 0 to 234 ± 25.5, 149.5 ± 20.5 and 33 ± 18.4 at day 4 for the 1.0, 0.2 and 0µM cultures, respectively. These values represent an increase of 1370% in the 1.0µM culture, 880% in the 0.2µM culture and 190% in cells containing one or more NPB in the 0µM condition (Table 5.3B).

The frequency of cells containing one or more NBud increased in the 1.0µM culture from zero at day 0, to 13 at day 4. The frequency in the 0.2µM 5azadC culture increased to 9 ± 1.4 at the same time point, while in the 0µM culture the frequency of cells with one or more NBud at day 4 was 1.5 ± 2.1 (Table 5.3C).

Analysis by two-way ANOVA of the frequency of BN cells containing one or more of each DNA damage biomarker (MNi or NPB or NBud) indicated that 31.4% of the variance was attributable to 5azadC concentration ($p < 0.0001$). 42.3% was attributable to time ($p < 0.0001$), and 24.7% of the observed variance was due to the interaction of 5azadC treatment with time ($p < 0.0001$) (Table 5.3D).

TABLE 5.3 Frequency of cells displaying one or more of the chromosomal damage biomarkers scored in the CBMN Cyt assay in the binucleated (BN) subset of WIL2-NS cells following culture in medium containing 0, 0.2 or 1.0μM 5-aza-2'-deoxycytidine (5azadC) over 4 days. Frequency per 1000 BN cells that contained (A) one or more micronuclei (MNi), (B) one or more nucleoplasmic bridge (NPB), (C) one or more nuclear bud (NBud), and (D) one or more of any DNA damage biomarker (MN or NPB or NBud). (Mean ± SD (n = 2) for each 5azadC concentration at each time point. P values represent analysis by two-way ANOVA. Data not sharing the same superscript letter within each time point differ significantly from each other, as measured by the Bonferroni post test).

		[5azadC] in medium (μmol/L)			
	Time	0	0.2	1.0	
(A) Frequency of BN with 1 or more MNi	Day 0	17.0 ± 1.4	17.0 ± 1.4	17.0 ± 1.4	Effect of time $p < 0.0001$
	Day 1	15.0 ± 12.7	18.5 ± 7.8	22.5 ± 4.9	
	Day 2	17.0 ± 1.4^{b}	40.5 ± 2.1^{b}	87.0 ± 18.4^{a}	
	Day 3	11.0 ± 2.8^{c}	77.5 ± 4.9^{b}	103.5 ± 6.4^{a}	
	Day 4	6.5 ± 2.1^{b}	79.5 ± 0.7^{a}	103.0 ± 19.8^{a}	
		Effect of 5azadC $p < 0.0001$			Interaction $p < 0.0001$
(B) Frequency of BN with 1 or more NPB	Day 0	17 ± 4.2	17 ± 4.2	17 ± 4.2	Effect of time $p < 0.0001$
	Day 1	20 ± 8.5	39 ± 15.6	18 ± 0.0	
	Day 2	26 ± 8.5^{b}	43 ± 4.2^{b}	109 ± 9.9^{a}	
	Day 3	22 ± 8.5^{c}	146 ± 17.0^{b}	204 ± 42.4^{a}	
	Day 4	33 ± 18.4^{c}	149.5 ± 20.5^{b}	234 ± 25.5^{a}	
		Effect of 5azadC $p < 0.0001$			Interaction $p < 0.0001$
(C) Frequency of BN with 1 or more NBud	Day 0	0 ± 0.0	0 ± 0.0	0 ± 0.0	Effect of time $p < 0.0001$
	Day 1	0.5 ± 0.7	0 ± 0.0	3 ± 1.4	
	Day 2	0 ± 0.0^{b}	4 ± 1.4^{b}	14 ± 8.5^{a}	
	Day 3	1 ± 1.4^{b}	13 ± 0.0^{b}	10 ± 1.4^{a}	
	Day 4	1.5 ± 2.1^{b}	9 ± 1.4^{b}	13 ± 0.0^{a}	
		Effect of 5azadC $p < 0.0001$			Interaction $p = 0.0037$
(D) Frequency of BN with 1 or more DNA damage biomarker	Day 0	34.0 ± 5.7	34.0 ± 5.7	34.0 ± 5.7	Effect of time $p < 0.0001$
	Day 1	35.5 ± 3.5	57.5 ± 7.8	43.5 ± 6.4	
	Day 2	43.0 ± 9.9^{b}	87.5 ± 4.9^{b}	210 ± 0.0^{a}	
	Day 3	34.0 ± 4.2^{c}	236.5 ± 21.9^{b}	317.5 ± 50.2^{a}	
	Day 4	41.0 ± 18.4^{c}	238.0 ± 18.4^{b}	350.0 ± 45.3^{a}	
		Effect of 5azadC $p < 0.0001$			Interaction $p < 0.0001$

5.3.3.2 Total number of DNA damage biomarkers per 1000 BN cells

The results presented in the previous section (5.3.3.1) show the frequency of BN cells with one or more of the biomarkers of DNA damage examined in the CBMN Cyt assay (MNi, NPB, NBuds), per 1000 BN cells. The total number of each of these biomarkers, however, is typically higher than the data presented in 5.3.3.1 because an individual BN cell may display multiple DNA damage events (see examples in Figure 3.5). Accordingly, the actual number of DNA damage biomarkers present per 1000 BN is presented in this section, and in Figure 5.7. The data presented here shows the total number of each biomarker (MNi, NPBs or NBuds, individually, and collectively) recorded per 1000 BN cells, at each time point for each 5azadC concentration over 4 days.

The total number of MNi recorded per 1000 BN increased from 18.5 ± 2.1 at day 0 to 147.5 ± 30.4 after four days in 1.0µM 5azadC, an increase of almost 800% relative to control cultures. The increase in MNi was statistically significant with two-way ANOVA analysis indicating 35.5% of the variance was attributable to 5azadC concentration ($p < 0.0001$) and 35% to time ($p < 0.0001$). The interaction of 5azadC and time explained 25.9% of the observed variance ($p < 0.0001$) (Figure 5.7A).

The total number of NPB (per 1000 BN cells) increased significantly from day 0 (19.0 ± 4.2), to 193.4 ± 34.8 (an increase of over 1000%) and 317 ± 66.5 (an increase of 1668%) respectively, in cells grown in 0.2µM and 1.0µM 5azadC for 4 days (Figure 5.7B). Two-way ANOVA analysis showed 25% of the variance observed was due to the interaction of 5azadC concentration with time ($p < 0.0001$), while 5azadC alone was responsible for 26.9% of the variance ($p < 0.0001$), and 43.8% was due to time ($p < 0.0001$). The number of NPBs observed after 4 days in culture with 1.0µM 5azadC treatment was approximately 3-fold higher than the numbers observed previously in cells grown in 30nM FA for 42 days (see Figure 4.11B). There were 110 NPB per 1000 BN cells grown under conditions of severe FA-insufficiency for 42 days, compared with 317 NPB per 1000 BN cells after culture in 1.0µM 5azadC for only 4 days.

A significant increase in the frequency of NBuds was also recorded in a dose and time-dependent manner. Similar but delayed increases were seen in the cells cultured in 0.2µM 5azadC. Concentration of 5azadC was shown to be responsible for 29.7% of the observed variance ($p < 0.0001$), 36.4% to time ($p < 0.0001$), and 24.7% of the variance was attributable to the interaction of 5azadC concentration with time ($p = 0.004$) (Figure 5.7C).

Analysis by two-way ANOVA of the total number of DNA damage events per 1000 BN (calculated by combining total MNi, NPBs and NBuds) showed highly significant differences between conditions over time. Of the observed variance, 30.3% was attributable to 5azadC concentration in medium ($p < 0.0001$), whereas 41.3% was due to time ($p < 0.0001$) and 25% to the interaction of treatment and time ($p < 0.0001$) (Figure 5.7D).

The relationship between TL and the biomarkers of DNA damage was examined by calculating the areas under the curves for TL for each condition with time (as presented in Figure 5.4) (AUC TL), and areas under the curves for each biomarker with time, as presented in Figure 5.7A-C. Strong, positive relationships were observed between AUC TL and AUC for each individual DNA damage biomarker; AUC TL vs AUC MNi (Pearson's $r = 0.88$, $p = 0.02$), AUC TL vs AUC NPB ($r = 0.9$, $p = 0.01$), AUC TL vs AUC NBud ($r = 0.88$, $p = 0.02$) (Table 5.4). The correlation between AUC TL and AUC total DNA damage biomarkers (total MNi plus NPB plus NBuds (obtained from Figure 5.7D)) resulted in a Pearson's r value of 0.89 ($p = 0.02$) (Table 5.4 and Figure 5.8).

The relationship between 5azadC concentration in medium with each biomarker of DNA damage was examined by calculating the areas under the curves (AUC) for each biomarker with time, as presented in Figure 5.7A-C. Each of these relationships was found to be positive and significant; 5azadC vs AUC MNi ($r = 0.9$, $p = 0.02$); 5azadC vs AUC NPB ($r = 0.9$, $p = 0.01$), 5azadC vs AUC NBud ($r = 0.89$, $p = 0.02$) (Table 5.5). AUC for the total number of DNA damage biomarkers (Figure 5.7D) correlated with 5azadC concentration, resulted in a Pearson's r value of 0.9 ($p = 0.01$) (Table 5.5 and Figure 5.9).

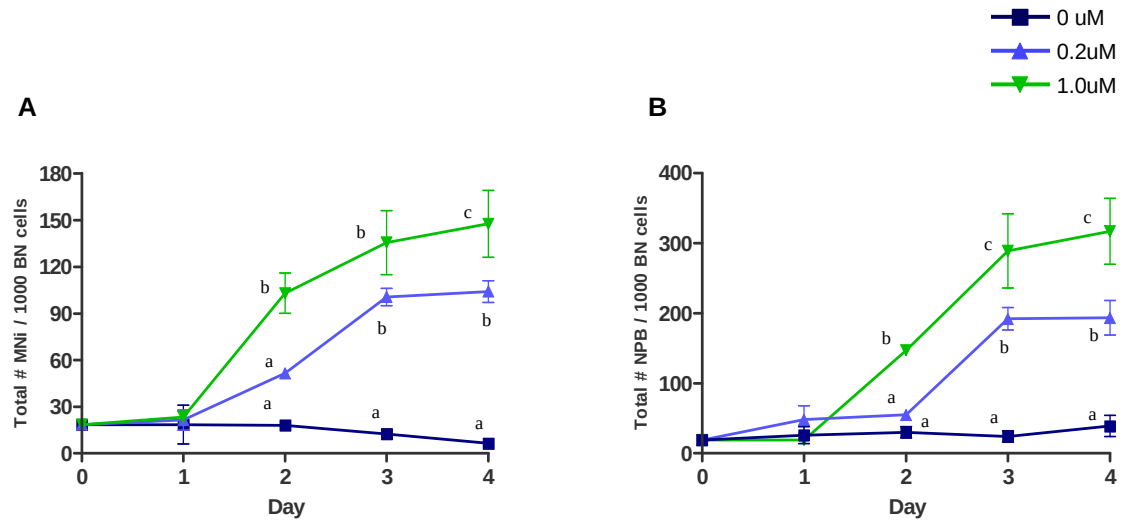

Source of variation	% of total variation	P value
Interaction	25.86	< 0.0001
5azadC	35.46	< 0.0001
Time	34.92	< 0.0001

Source of variation	% of total variation	P value
Interaction	25.01	< 0.0001
5azadC	26.87	< 0.0001
Time	43.84	< 0.0001

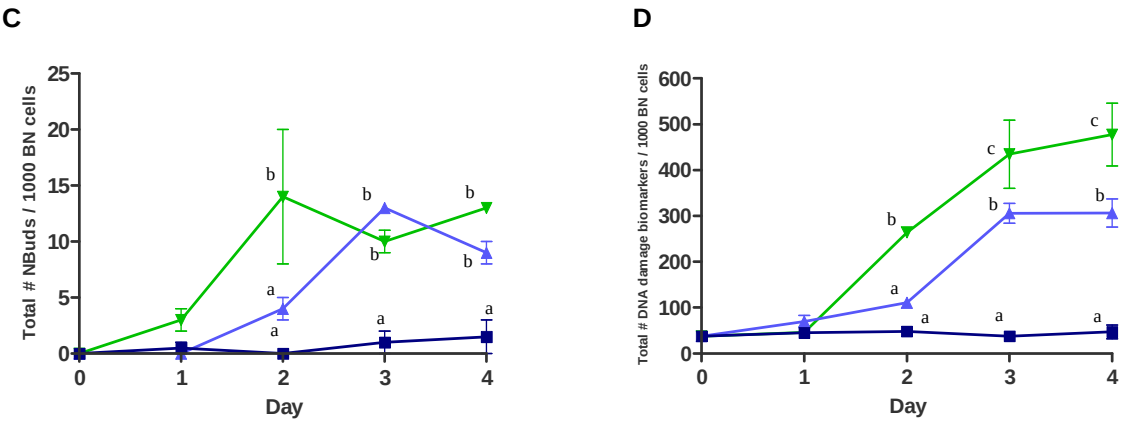

Source of variation	% of total variation	P value
Interaction	24.65	0.0037
5azadC	29.73	< 0.0001
Time	36.36	< 0.0001

Source of variation	% of total variation	P value
Interaction	25.02	< 0.0001
5azadC	30.30	< 0.0001
Time	41.31	< 0.0001

Figure 5.7 Chromosomal damage, measured by the CBMN Cytome assay, in WIL2-NS cells grown in complete medium containing 0, 0.2 or 1.0μM 5-aza-2'-deoxycytidine (5azadC) for 4 days. Data represent the total number of DNA damage biomarker events present per 1000 BN cells. (A) Total micronuclei (MNi); (B) Total nucleoplasmic bridges (NPB); (C) Total nuclear buds (NBud); and (D) Total number of damage events in 1000 BN cells (total MNi, NPB and NBuds combined) (N = 2. Error bars indicate SD. Groups not sharing the same letter at each time point differ significantly from each other, as measured by the Bonferroni post-test. Data tables represent results of analysis by two-way ANOVA).

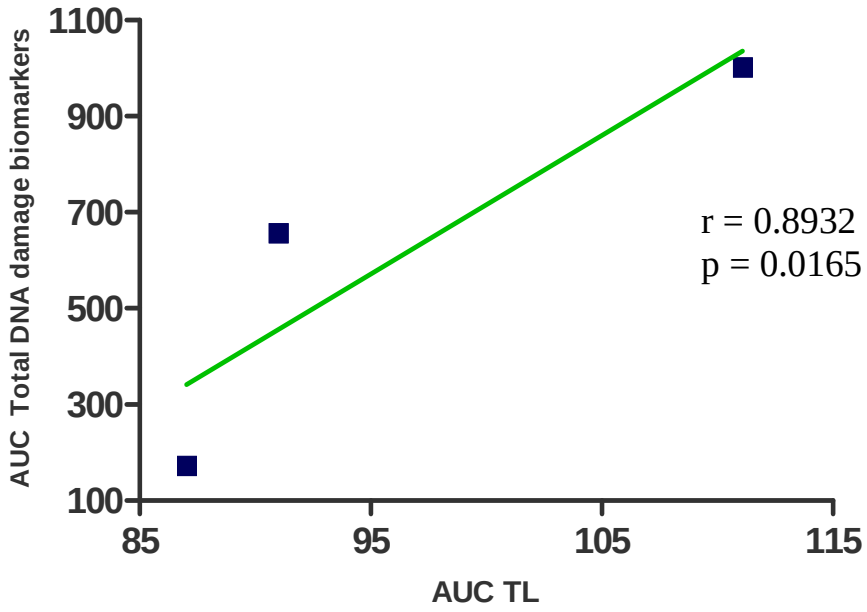

Figure 5.8 Correlation between area under the curve (AUC), comparing telomere length (AUC TL) and AUC total DNA damage biomarkers. Areas were obtained from Figures 5.4 and 5.7D respectively.

Table 5.4 Correlations between AUC TL and AUC MNi, AUC NPB and AUC NBuds (individually and combined, per 1000 BN cells) in WIL2-NS cells following 4 days culture in complete medium containing either 0, 0.2 or 1.0µM 5azadC. Areas were obtained from Figures 5.4 and 5.7A-D.

	Pearson's r	P value
Total MNi	0.8790	0.0211
Total NPB	0.9014	0.0141
Total NBuds	0.8765	0.0219
Total damage markers	0.8932	0.0165

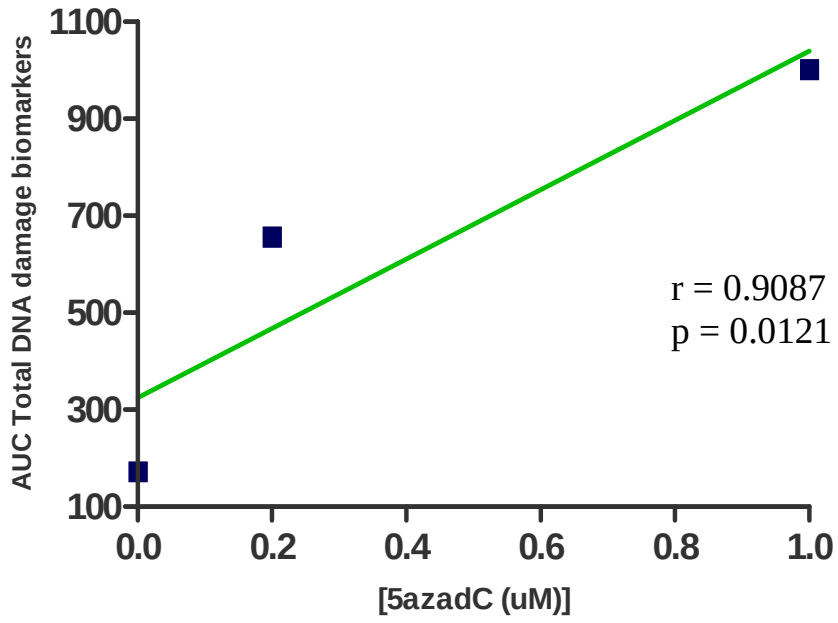

Figure 5.9 Correlation between 5azadC concentration in medium (µM) and AUC frequency of total DNA damage biomarkers in WIL2-NS cells following 4 days culture in complete medium containing either 0, 0.2 or 1.0µM 5azadC. Areas were obtained from Figure 5.7D.

Table 5.5 Correlations between 5azadC concentration in medium (µM) and AUC frequency of MNi, NPB and NBuds (individually and combined, per 1000 BN cells) in WIL2-NS cells following 4 days culture in complete medium containing either 0, 0.2 or 1.0µM 5azadC. Areas were obtained from Figure 5.7A-D.

	Pearson's r	P value
Total MNi	0.8955	0.0158
Total NPB	0.9163	0.0102
Total NBuds	0.8931	0.0165
Total damage markers	0.9087	0.0121

5.3.3.3 Cells exhibiting multiple NPB ("Chewing-gum" cells)

A novel observation during the scoring of the DNA damage for the current experiment was the high frequency of BN cells exhibiting unusual nuclear morphology, with multiple and/or wide connections between the nuclei. The appearance suggested the presence of multiple NPBs, possibly due to the presence of several dicentric chromosomes that inhibit separation of the two daughter nuclei at anaphase. This effect created a "chewing gum"-like appearance (Figure 5.6 C-F). Where these morphologies occurred, individual NPBs could not be resolved for scoring purposes. Accordingly, these cells were excluded from scoring in the CBMN Cyt assay, because the structures did not meet the standard criteria for NPBs defined within the CBMN Cytome assay (Chapter 3.3.6.6) which state that an NPB must have the following characteristics[14]:

- The width of an NPB may vary considerably but usually does not exceed 1/4th of the diameter of the nuclei within the cell.
- NPBs should also have the same staining characteristics as the main nuclei.
- On rare occasions more than one NPB may be observed within one BN cell (Figure 5.6A and B).
- A BN cell with one or more NPB may also contain one or more MNi (see example in Figure 3.5E).

The NPB data presented in this chapter (5.3.3.1 and 5.3.3.2 above) relate only to NPBs scored using the standard criteria for the CBMN Cyt assay (as defined above). It should be noted, therefore, that these data may underestimate the total number of nucleoplasmic bridges in these samples. As such, detailed analysis of total NPB, incorporating these novel morphologies (which were scored notionally as BN cells containing 5 NPBs), was undertaken.

These data are presented and discussed separately in Chapter 6 of this thesis.

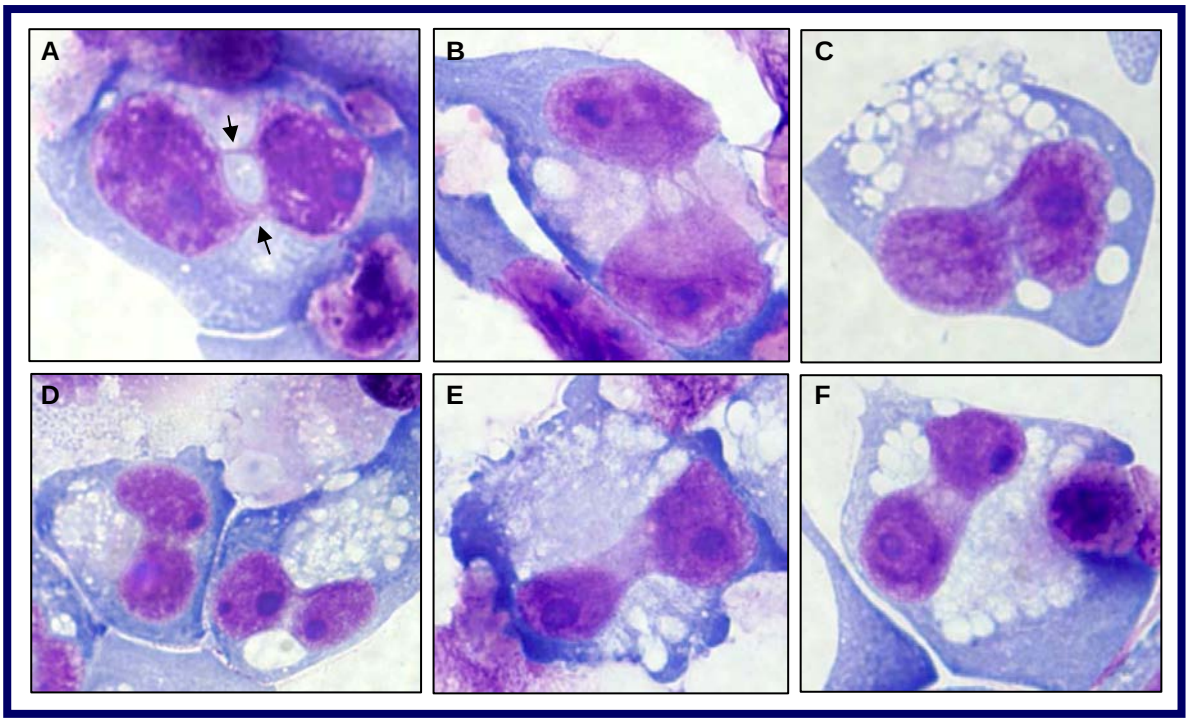

Figure 5.6 Representative photomicrographs of NPBs in WIL2-NS cells cultured for four days in medium containing 1.0μM 5azadC, blocked at the BN stage using cytochalasin-B. A high proportion of the BN and multinucleated cells grown in the presence of 5azadC displayed multiple NPB. (A) An example of a BN cell displaying clearly identifiable NPBs. These NPBs meet the standard scoring criteria for the CBMN Cyt assay and would have been recorded as two NPBs; (B) an example of a BN cell displaying multiple NPBs. This cell was scored as containing 4 NPBs. (C-F) Some BN cells appeared to have so many NPB that they displayed a "chewing-gum" effect, where the two nuclei were unable to separate at anaphase. In these cases, the NPB were not clearly discernible for scoring and they did not meet the standard scoring criteria. Such cells were scored as containing a notional '5' NPB per BN cell (1000x magnification).

5.4 DISCUSSION

5.4.1 Impact of 5azadC treatment on telomere length

This study explored the primary hypothesis that hypomethylation of DNA, induced by inhibition of DNMT, results in an increase in telomere length (TL) under conditions of folate sufficiency. The hypothesis was supported by the observation that TL in WIL2-NS cells increased following exposure to the DNMT inhibitor, 5azadC. The increase was significant after 24 hours, was followed by a small reduction and was then maintained at a constantly raised level through to the completion of the study at day 4. The elongation of telomeres occurred in a dose dependent manner. A significant, positive correlation was observed between the concentration of 5azadC in medium and the area under the curve when TL was plotted against time, suggesting that DNA hypomethylation may result in longer telomeres. This observation is consistent with the findings of the studies into the effects of FA-deficiency (Chapter 4), where the greatest elongation of telomeres was observed under the most severe conditions of FA deficiency (most hypomethylating). These findings are also consistent both with the work of Gonzalo *et al* (2006), in which mouse ES cells genetically deficient in DNMT were found to have significantly longer telomeres than wild-type cells[328]. Furthermore, a recently published study showed that epigenetic changes affected TL in neoplastic cells[319]. The latter study, using a panel of cancer cell lines, found a correlation between TL and levels of DNA methylation, including global, pericentromeric, and subtelomeric methylation[319]. In particular, subtelomeric hypomethylation had a strong negative association with increased telomere content[319]. The researchers confirmed that neither the expression, nor activity, of the telomerase enzyme was responsible for the increase in TL[319].

The effects of FA-deficiency on telomere length (discussed in Chapter 4) were elongation in the short term, followed by a significant decrease over the longer term. It was proposed that the longer-term loss of telomere content was possibly due to incorporation of uracil into telomere sequences, resulting in double strand breakage and deletion of parts of the telomeres. The short term elongation, however, may have been due to loss of methylation at the subtelomere. To isolate the effect of methylation from the effect of uracil incorporation, 5azadC was used in this study was to selectively induce de-methylation of DNA. It was, therefore, anticipated that de-methylation induced by treatment with 5azadC, would not by itself lead to loss of TL over time. The results supported this proposal, as TL increased and then remained constant from day 2 through to the end of the experiment at day 4. However, while this finding suggests that DNA hypomethylation alone does not cause a reduction of telomere content in the longer term, it cannot be concluded that the late TL shortening

observed under conditions of severe folate insufficiency was due to incorporation of uracil into the telomere sequences. In addition, there is a large difference in time frame between the two studies, with only four days exposure to 5azadC, compared with 21 and 42 days exposure to folate deficiency. A further study is necessary, possibly using lower concentrations of 5azadC, to assess the relevance of exposure. It would also be interesting to assess the effects of simultaneous exposure to FA-deficiency and 5azadC, and whether the two treatments interact.

5.4.2 5azadC treatment and chromosome instability

The second hypothesis for this study was that DNA hypomethylation leads to an increase in chromosomal instability (CIN). The results supported this hypothesis, with dose-dependent increases in both the frequency of BN cells containing one or more damage biomarkers (MNi, NPB, NBud), and the total number of damage events per thousand BN cells. Strong positive correlations were observed between the AUC total number of DNA damage biomarkers with both AUC TL and 5azadC concentration in medium. The increase in MNi, indicating double strand breakage of DNA with resultant chromosome breakage or loss[14], may suggest higher order structural changes to chromatin that result in loss of overall stability. Early studies on the effects of 5azadC showed that there was an increase in single and double strand breaks, together with de-condensation of genetically inactive chromatin, after only a few hours of exposure to the compound[356]. A more recent detailed examination of the mechanisms of cytotoxicity of both 5azaC and 5azadC has provided evidence that these drugs cause damage and instability in chromosomes, and affect the capacity of the cell to respond to damage[357]. The latter study showed that 5azadC treatment leads to robust induction of γ-H2AX (an early marker of double strand breakage (DSB)), DNA fragmentation and activation of DNA repair proteins in both the ATM and ATR pathways. It was also found that DNMT1 co-localised with γ-H2AX, demonstrating for the first time the presence of DNMT1 at sites of DNA damage in 5azadC-treated cells. Cells lacking DNMT1 were shown to be deficient in their ability to induce γ-H2AX, and they exhibited altered induction of other DNA repair proteins, suggesting that DNMT1 may be an active component of the DNA damage response system[357]. It is pertinent that the concentration of 5azadC found by Pallii[357] to induce γ-H2AX foci and DNA strand breakage was at or below 1μM, which was the highest concentration used in the study reported in this chapter. The significant increase in MNi observed in cells treated in 0.2 or 1.0μM 5azadC herein is consistent with the known genotoxic mechanisms of this drug[357]. Additionally, it is also plausible that hypomethylation may have affected expression of genes responsible for maintaining chromosome stability, and potentially telomere structure.

As discussed previously, nuclear buds (NBuds) are believed to expel amplified genetic material from the genome. This elimination process is understood to involve recombination between homologous regions and the formation of the amplified sequences into mini-circles[14,15]. The increase in NBuds observed previously under conditions of FA deficiency (Chapter 4), and here after inhibition of DNMT with 5azadC, suggests that recombination may be up-regulated under conditions of hypomethylation. Other studies have reported significant increases in telomeric sister chromatid exchange (T-SCE) when DNA methylation is reduced[319,328], while earlier studies investigating the effect of 5azadC on genome stability found a heritable increase in amplified genes[356]. In the latter study, the authors proposed that the observed increase in amplification was not a transient stress response, but an increase in non-homologous unequal SCE, and that this gave rise initially to duplication events, which were then rapidly amplified during DNA replication[356]. While these authors did not specify whether telomeric DNA was involved in the SCE events, the observation of increased SCE in the presence of 5azadC is consistent with the more recent findings of Vera *et al* (2008) who showed that there were significant increases in T-SCE in neoplastic cells following treatment with 5μM 5azadC for 72 hours[319]. These authors also showed that hypomethylation of the subtelomere was strongly correlated with the significant increase in T-SCE[319]. These findings suggest that drugs that cause a reduction in DNA methylation may lead indirectly to recombination, and thence to disruption of telomere length homeostasis[319].

The strong increase in NBuds observed herein in response to treatment with 5azadC, and the evidence of others suggesting that SCE may be responsible for gene amplification, suggests that the alternative mechanism of telomere lengthening (ALT) may have been activated in the 5azadC-treated cells. Gonzalo *et al* demonstrated high levels of recombination due to SCE involving telomeric sequences in murine ES cells that were deficient in DNMT[328]. In addition, these cells were found to contain ALT-associated promyelocytic leukaemia (PML) bodies (APBs)[328], which are known to contain extrachromosomal telomeric DNA, telomere-specific binding proteins, and proteins involved in DNA recombination and replication[358]. The presence of APBs led the authors to propose that DNA methylation status regulates ALT[148,328]. Further evidence to support this hypothesis was provided by Vera *et al* (2008), who demonstrated that methylation of subtelomeric DNA was correlated negatively with both TL and with telomeric sister chromatid exchange (T-SCE) events[319]. As a result, Tilman *et al* explored whether DNA hypomethylation of chromosome ends contributed to ALT by facilitating SCE events involving telomeric sequences (T-SCEs)[359]. These researchers found conflicting results in different cell types, with high levels of T-SCE and the presence of ALT correlating positively with hypomethylation of subtelomeric sequences in some cells, but

negatively in others[359]. Moreover, expression of active telomerase in ALT tumor cells reduced T-SCE efficiently, despite subtelomeric sequences remaining hypomethylated[359]. Overall, these findings suggest that although sub-telomeric DNA hypomethylation often coincides with the ALT process in human tumor cells, it is not obligatory for T-SCE[359].

Interestingly, while the numbers of MNi and NBuds observed after treatment with 5azadC for only four days were similar to those observed after 42 days of folate insufficiency, the mean number of NPBs was up to three-fold higher in the cells treated with 5azadC. In addition, many 5azadC-treated cells exhibited multiple NPBs, resulting in what could be described as a "chewing gum" effect when the two daughter nuclei attempted to separate. As shown previously[6,276,332], frequency of NPBs increases when telomeres are shortened and/or compromised. This suggests that the high level of NPBs observed herein are likely due to compromised telomere ends, leading to end fusions and the formation of dicentric chromosomes. The latter then present as NPBs in binucleated (BN) cells trapped at anaphase, because the chromosomes are unable to separate. In cells that have not been blocked at the BN stage, dicentric chromosomes will break unevenly at anaphase, resulting in the daughter nuclei receiving abnormal gene dosage. Uncapped chromosome ends lack protection and are likely to fuse again with another chromosome, thus causing the process to cycle and lead to increasing levels of genomic disarray and instability. This is the breakage-fusion-bridge (BFB) cycle, which has been shown to be an early event after telomere loss and to lead to amplification of genes (including oncogenes)[33]. Consistent with the findings of Haaf *et al* (1995) in cells treated with 5azadC, Lo *et al* demonstrated that BFB cycles can last for many generations after the initial sister chromatid fusion[33,356]. The findings in this thesis are also consistent with those of Gisselsson *et al* (2005), who found an increased frequency of NPB in ICF cells that lack genes encoding DNMT3b[347].

5.5 CONCLUSIONS

- These findings, that short-term treatment of WIL2-NS cells with 5azadC treatment leads to elongation of telomeres, supports the original hypothesis. The proposal that hypomethylation alone, without the confounding influence of uracil incorporation, will lead to elongated TL was also supported. However, the studies using 5azadC were short term (up to four days), while the studies on cells exposed to folate insufficiency were longer term and extended up to 42 days.

- The second hypothesis for this part of the study, that reduced DNA methylation arising from DNMT inhibition, will result in increased chromosomal instability was also supported. The possibility remains, however, that the observed damage is a result of other cytotoxic effects of 5azadC, in addition to hypomethylation.

5.6 FUTURE DIRECTIONS

- Further studies are needed to explore whether 5azadC and/or FA deficiency cause subtelomeric hypomethylation, and whether these data correlate with LINE1 global methylation levels.

- Fluorescence *in situ* hybridisation (FISH) could be used to provide information regarding the presence of interstitial telomeric DNA in chromosomes, as well as showing whether MNi, NPBs and NBuds contained broken telomere fragments and/or amplified telomeric DNA. Centromeric probes would also allow the origin of MNi to be determined.

- In addition, FISH could be used to explore whether there is activation of ALT, via the presence of APBs, both in WIL2-NS cells, and in WIL2-NS cells exposed to 5azadC and/or FA-deficiency.

- Telomeric sister chromatid exchange (T-SCE) studies could be used confirm whether global and/or subtelomeric hypomethylation leads to telomeric recombination of chromosomes.

CHAPTER 6:
THE RELATIONSHIP BETWEEN TELOMERE LENGTH, GLOBAL DNA HYPOMETHYLATION, URACIL INCORPORATION IN THE TELOMERE AND NUCLEOPLASMIC BRIDGE FORMATION

6 THE RELATIONSHIP BETWEEN TELOMERE LENGTH, GLOBAL DNA HYPOMETHYLATION, URACIL INCORPORATION IN THE TELOMERE AND NUCLEOPLASMIC BRIDGE FORMATION

6.1 INTRODUCTION

Results presented in this thesis demonstrated that (i) FA insufficiency caused an increase in TL in WIL2-NS in the short term (Chapter 4), and (ii) treatment with DNMT inhibitor, 5-aza-2'-deoxycytidine (5azadC) (Chapter 5), showed a rapid, sustained increase in TL in a dose dependent manner, suggesting that DNA hypomethylation results in telomere elongation. Previous studies have found that hypomethylation of subtelomeric DNA leads to increased recombination and sister chromatid exchange involving telomere DNA sequences (T-SCE)[319,328]. This mechanism may result in dicentric chromosome formation arising from end-to-end fusions, leading to an increase in nucleoplasmic bridges (NPB) and gene amplification[276]. The significant increase in NPBs and NBuds (a biomarker of gene amplification) in both the FA and 5azadC experiments provide further support, indirectly, for the hypothesis that subtelomeric hypomethylation may be an underlying mechanism for these forms of damage. Accordingly, it was important to compare levels of methylation in the FA deficiency and 5azadC treated WIL2-NS cells relative to controls to confirm whether methylation status was impacted by these treatments.

Long interspersed nuclear elements (LINEs) are retrotransposons, copies of which constitute approximately 20% of the human genome[311]. Around one million copies of intact LINE1 elements (the major LINE repeat) are present in the human genome. These sequences, which are approximately 6kb in length, are transcribed to RNA, then converted back to DNA by a reverse transcriptase prior to integration into the genome[311]. In somatic cells DNMT enzymes are responsible for maintaining methylation of the 5' position on the pyrimidine ring of cytosine residues within the LINE1 sequences. For this reason, a significant proportion of LINE1 sequences are located within regions of inactive chromatin[311]. Previous findings have shown that both global and subtelomeric methylation status correlate negatively with telomere length and increased T-SCE[319]. As similar correlations were not observed for global and pericentromeric methylation, the former suggests that global methylation status may be

inclusive of methylation status at the subtelomere[319]. Accordingly, it was speculated that measurement of global methylation of LINE1 sequences in the FA and 5azadC treated cells may provide useful information regarding the probable methylation status of the subtelomere in these samples.

Results from the FA deficiency studies presented in Chapter 4 (Figure 4.5) demonstrated a rapid, sustained decrease in TL in WIL2-NS after day fourteen. It was hypothesised that the loss of TL may have been due to double strand breakage arising from uracil incorporation. The significant, dose-dependent increase in MNi supported this theory indicating increased chromosomal breakage, although MNi may also have arisen from chromosome loss arising from unrelated mechanism(s) such as hypomethylation of centromeric DNA[54]. To investigate this hypothesis further, it was important to compare the relative levels of uracil in the telomeres of WIL2-NS cells cultured in the different FA and 5azadC concentrations

To further investigate the mechanism underlying the increase in telomere length under hypomethylating conditions it was also necessary to explore the high number of NPBs observed in WIL2-NS cells maintained in low FA and high 5azadC cultures. NPBs are indicative of dicentric chromosomes arising from either dysfunctional telomeres (resulting in end-to-end fusions) or misrepair of chromosome breaks. Unprotected telomere ends may arise from double strand (ds) breakage, BFB cycles, or from compromised telosome protein capping. The latter may be caused by reduced binding of TRF1 and TRF2 complexes when the telomere sequence is disrupted by adducts or abasic sites[139], an effect which is hypothesised may also occur with uracil incorporation into the telomere sequence. Accordingly, additional analyses were conducted to compare the frequency of binucleated (BN) cells containing multiple NPBs in the different treatments.

6.1.1 Aims

1. To compare global DNA methylation, uracil incorporation into telomeric DNA and frequency of BN cells containing multiple NPBs in WIL2-NS cells cultured in complete medium containing 30, 300, or 3000nM FA.
2. To compare global DNA methylation, uracil incorporation into telomeric DNA and frequency of BN cells containing multiple NPBs in WIL2-NS cells cultured in complete medium containing 0, 0.2 or 1.0µM 5azadC.
3. To explore the relationship between telomere length and global DNA methylation, uracil incorporation into telomeres and frequency of BN cells containing multiple NPB in WIL2-NS cells cultured in complete medium containing 30, 300, or 3000nM FA, and between WIL2-NS cells cultured in complete medium containing 0, 0.2 or 1.0µM 5azadC.

6.1.2 Hypotheses

1. Folate deficiency causes DNA hypomethylation, increased uracil in telomeres and a greater frequency of BN cells with multiple NPBs compared to folate replete conditions.
2. 5azadC causes DNA hypomethylation and an increased frequency of BN cells containing multiple NPB compared to controls. Uracil content in telomeric DNA remains unchanged by 5azadC treatment.
3. Telomere length is positively associated with DNA hypomethylation in WIL2-NS cells.
4. Telomere length is negatively associated with uracil in the telomere in WIL2-NS.
5. Frequency of BN cells containing multiple NPBs is positively associated with global DNA hypomethylation, and positively associated with increased uracil incorporation into telomeric DNA.

6.2 METHODS

DNA was isolated from WIL2-NS cells (method detailed at Chapter 3.5.1) at each time point of the long term (42-day) FA deficiency experiment (Chapter 4), and the 5azadC experiment (Chapter 5). Cells from each sample point for these experiments had previously been frozen and stored in liquid nitrogen (Chapter 3.2.4). Isolated DNA was then stored at 4°C for qPCR assays to assess levels of global methylation (Chapter 3.5.3) and uracil incorporation into the telomere (Chapter 3.5.2).

6.2.1 Assessment of global hypomethylation

Hypomethylation of LINE1 repeating sequences, relative to that of day 0 samples, was used to provide an indication of the change in global (and thus subtelomeric) methylation status following FA or 5azadC treatments. These assays were conducted by Dr. Varinderpal Dhillon and Ms. Susan Mitchell at the CSIRO laboratories in North Ryde, Sydney, NSW, and the data presented as part of this thesis. All analyses were conducted by the author. Detailed methodology is provided at Chapter 3.5.3. In brief, sample DNA, together with 100% unmethylated and 100% methylated DNA standards (purchased commercially), were pre-treated with sodium bisulphite to convert unmethylated cytosine residues to uracil. This pre-treatment exploits the different sensitivities of cytosine and 5-methylcytosine (5-MeC) to deamination by bisulphite under acidic conditions, with all cytosine residues being converted to uracil, while 5-MeC remains unchanged[312]. Sample DNA, and the standards, are then amplified in the presence of primers specific to the LINE1 sequence. Where cytosine has been converted to uracil, thymidine will be incorporated in subsequent cycles. This will, in turn, base pair with adenosine, altering the LINE1 sequence. The changed sequence causes reduced binding affinity for the LINE1 specific primers, leading to a reduction in amplified product, with Cq values increasing with increasing hypomethylation.

Bisulphite-treated DNA (10ng) was dispensed into each well of a 96 well plate along with 18µl of master mix containing SYBR Green, nucleotides and Taq polymerase. All samples were run in duplicate and Cq values obtained for sample and standard DNA. A standard curve was then prepared using the Cq values from the commercial standards, and their dilutions. DNA concentrations for each 2µl DNA sample were normalised by quantifying ribosomal DNA using a separate set of primers in a separate reaction plate. Ratios were calculated for hypomethylation of each normalised sample, and these data were then converted to a value relative to LINE1 hypomethylation of the day 0 control sample, which was recorded as 1.0.

6.2.2 Quantification of uracil in telomeric sequences

The amount of uracil in the telomere of each sample from the long term FA study and the 5azadC study was measured by a novel qPCR method conceived and developed by Prof Michael Fenech and Dr Nathan O'Callaghan, in this laboratory. Full detail of the method is provided at Chapter 3.5.2. In brief, DNA samples were established in paired wells of a 96-well plate. Uracil glycosylase and buffer, was added to one well, while buffer only was added to the paired well. Plates were prepared on ice, followed by incubation for three hours at 37°C, 5 minutes at 80°C to denature the enzyme, and then stored at 4°C. Cq was then assessed using qPCR in both the digested and undigested DNA samples. All samples were run in duplicate. The assay is based on the fact that uracil in DNA is cleaved by uracil glycosylase, resulting in an abasic site[74]. When an abasic site is encountered Taq polymerase activity will either be slowed or stopped during the PCR reaction. As a result the Cq value for the digested sample will be higher relative to the undigested sample. The more uracil that is present in the original (sample) template DNA, the more abasic sites will be generated by uracil glycosylase digestion. This will then be reflected as a higher Cq value relative to undigested, paired samples. The difference between the Cq values for the digested and the undigested DNA reflects the amount of uracil present in the original sample. Results were then converted to a percentage relative to the amount of uracil present in day 0 samples, using the mean value from Day 0 as 100%.

It should be noted that the method used for the uracil analysis has not yet been fully optimised and continues to be refined. One component that is believed may increase assay sensitivity is the addition of an endonuclease following the digestion step, and this is currently being tested. As such, the results presented here should be viewed as preliminary.

6.2.3 Frequency of binucleated cells containing multiple NPB

To obtain more detailed data regarding number and frequency of NPB present in cells treated in the different FA and 5azadC conditions, additional scoring was undertaken on the same CBMN Cytome assay slides previously scored for these experiments (presented in Chapters 4 and 5). These slides were re-scored, recording the following:

(i) the frequency of BN containing 1, 2, 3 or 4 NPB (based on standard CBMN Cyt scoring criteria (Chapter 3.3.6.6));

(ii) the frequency of BN containing a number of NPB so high as to cause them to be indistinguishable as individual NPBs. The nuclear morphology of these cells is such

that it resembles “chewing gum” between the two nuclei as they have attempted to separate at anaphase; and

(ii) the total number of NPB in each treatment at each time point, including “chewing gum” cells which were scored as having ‘5’ NPBs. The latter had not been included in data presented in previous chapters as these morphologies did not meet the standard scoring criteria for inclusion in CBMN Cyt data (See Chapter 5.3.3.3).

For the FA experiment 1000 BN were scored per slide. For the 5azadC study, due to the low numbers of BN cells in the higher 5azadC dosage, 500 BN were scored per slide. For each study, two slides were scored for each treatment, at each time point.

6.3 RESULTS

6.3.1 Global DNA Methylation

6.3.1.1 Long term (42 day) folic acid study

Hypomethylation was calculated relative to that of the day 0 samples. Low FA impacted significantly on DNA methylation status in a dose-related manner, with increasing levels of global LINE1 hypomethylation occurring over the 42-day study. Analysis by two-way ANOVA indicated that 38.1% of the variance was attributable to FA concentration in medium ($p = 0.0007$), 17.6% was due to time ($p = 0.03$), whereas the interaction of FA and time was responsible for 28.1% of observed variance ($p = 0.03$) (Figure 6.1A).

Area under the curve for LINE1 hypomethylation with time (AUC LINE1 hypomethylation) was significantly and negatively correlated with FA concentration in culture medium ($r = -0.98$, $p = 0.0004$) (Figure 6.1B). AUC for TL with time (AUC TL (obtained from data in Figure 4.5)) was positively related to hypomethylation levels ($r = 0.85$, $p = 0.03$) (Figure 6.1C), as was the AUC total DNA damage biomarkers ($r = 0.99$, $p < 0.0001$) (Figure 6.1D). The latter was calculated based on the total number of damage events (MNi plus NPBs plus NBuds) present in 1000 BN cells, with time (obtained from Figure 4.11D).

6.3.1.2 5azadC study

A significant increase in global LINE1 hypomethylation was observed with increasing concentrations of 5azadC. Analysis by two-way ANOVA indicated 30.1% of the variance was attributable to 5azadC concentration in medium ($p = 0.002$), 20.9% was due to time ($p = 0.04$), and 25.3% of observed variance in hypomethylation was attributable to the interaction of both factors ($p = 0.1$) (Figure 6.2A).

AUC LINE1 hypomethylation was positively associated with the concentration of 5azadC in culture medium ($r = 0.99$, $p < 0.0001$) (Figure 6.2B). Significant, positive correlations were also observed between AUC LINE1 hypomethylation and AUC TL (obtained from data presented in Figure 5.4) ($r = 0.99$, $p < 0.0001$) (Figure 6.2C), and between AUC LINE1 hypomethylation and AUC total DNA damage biomarkers (data obtained from Figure 5.7D) ($r = 0.94$, $p < 0.0001$) (Figure 6.2D).

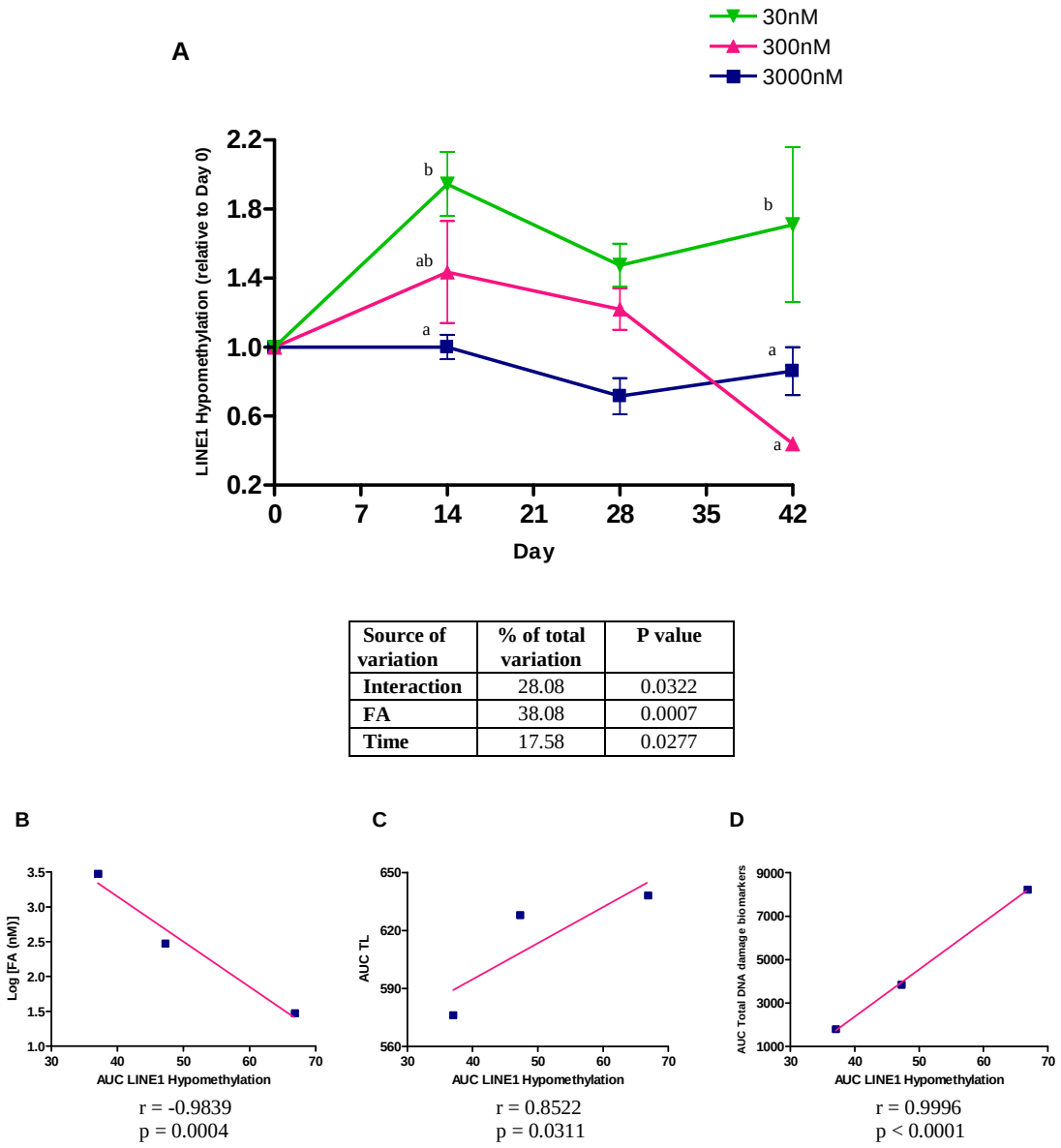

Source of variation	% of total variation	P value
Interaction	28.08	0.0322
FA	38.08	0.0007
Time	17.58	0.0277

Figure 6.1 Hypomethylation of LINE1 sequences in WIL2-NS cells cultured in medium containing either 30, 300 or 3000nM FA for 42 days. (A) Data is presented relative to the level of hypomethylation of Day 0 samples (set at 1.0). (Data table represents analysis by two-way ANOVA. N = 2 for each treatment at each time point. Error bars indicate SD. Points not sharing the same letter at each time point are significantly different from each other, as measured by Bonferroni post test). Correlation of AUC LINE1 hypomethylation with (B) FA concentration in culture medium; (C) AUC TL, and (D) AUC total DNA damage biomarkers. (AUC; area under the curve for the stated parameter, with time. BN; binucleated cells. In Figure 6.1D, total DNA damage biomarkers represents all MNi, NPBs and NBuds combined, per 1000 BN cells).

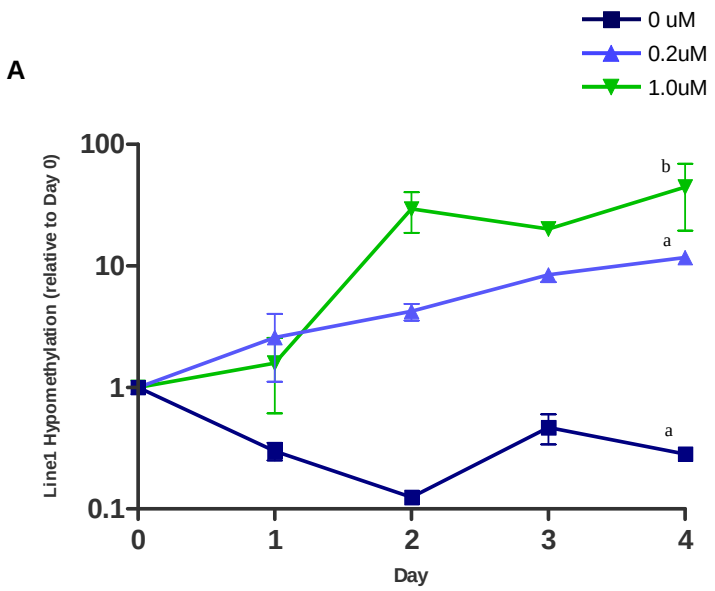

Source of variation	% of total variation	P value
Interaction	25.31	0.1160
5azadC	30.14	0.0021
Time	20.94	0.0387

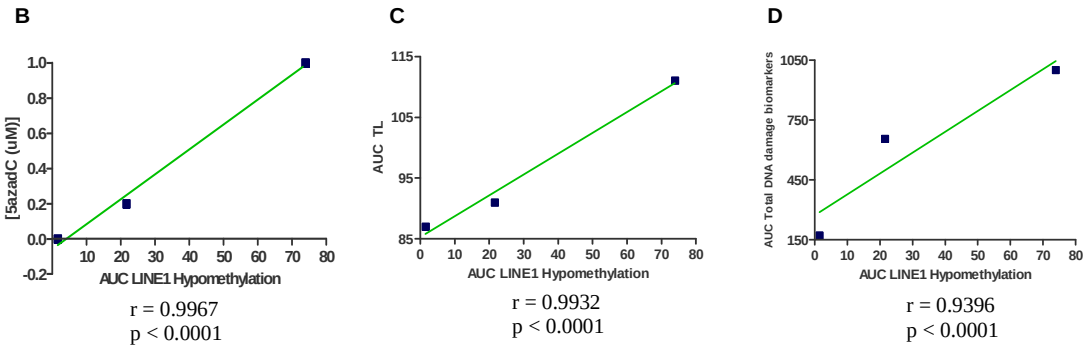

Figure 6.2 Hypomethylation of LINE1 sequences in WIL2-NS cells cultured in medium containing either 0, 0.2 or 1.0μM 5azadC for 4 days. Data is presented relative to the level of hypomethylation of day 0 samples (set at 1.0) (A). (Data table represents analysis by two-way ANOVA. N = 2 for each treatment at each time point. Error bars indicate SD. Data on the y axis is presented on a log scale. Points not sharing the same letter at each time point are significantly different from each other, as measured by Bonferroni post test). Correlation of AUC LINE1 hypomethylation with (B) 5azadC concentration in culture medium; (C) AUC TL, and (D) AUC total DNA damage biomarkers. (AUC is the area under the curve for the stated parameter, with time. BN; binucleated cells. In Figure 6.2D, total DNA damage events represents all MNi, NPBs and NBuds combined, per 1000 BN cells).

6.3.2 Uracil incorporation into telomeric DNA

6.3.2.1 Long term (42 day) folic acid study

The presence of uracil in telomeric DNA was measured at days 0, 28 and 42 of the long term FA study. Analysis of these data did not indicate significant differences between treatments. A trend was observed, however, for increasing uracil in the telomeres of cells cultured in lower FA conditions (30 and 300nM), compared with the 3000nM dose (Figure 6.3). At day 42 uracil in telomeric DNA of cells cultured in 30nM and 300nM FA treatments was 290% and 343% that of day 0, respectively. In contrast, at day 42 no uracil was recorded in telomeres of cells cultured in FA replete (3000nM) medium (Table 6.1A).

Analysis by two-way ANOVA of these data showed 2.3% of the variance was attributable to treatment ($p = 0.65$), 7.72% to time ($p = 0.26$) and 16.5% of the observed variance was due to interaction of both factors ($p = 0.2$).

The relationship between uracil content in telomeric DNA at day 42 with the concentration of FA in culture medium was negative, but failed to reach statistical significance ($r = -0.72$, $p = 0.11$) (data not shown). The correlation between uracil at day 42 and telomere length was negative, and non-significant ($r = -0.27$, $p = 0.59$) (data not shown).

6.3.2.2 5azadC study

Uracil content of telomeric DNA of cells cultured in medium containing 5azadC did not differ significantly from cells grown in control medium (0µM 5azadC), and no trends were evident between treatments (Table 6.1B).

Two-way ANOVA analysis of data showed only 1.4% of variance was attributable to treatment ($p = 0.45$), while 50.3% was due to time ($p < 0.0001$) and 9.6% of observed variance was attributed to the interaction of both factors ($p = 0.22$) (graph not shown).

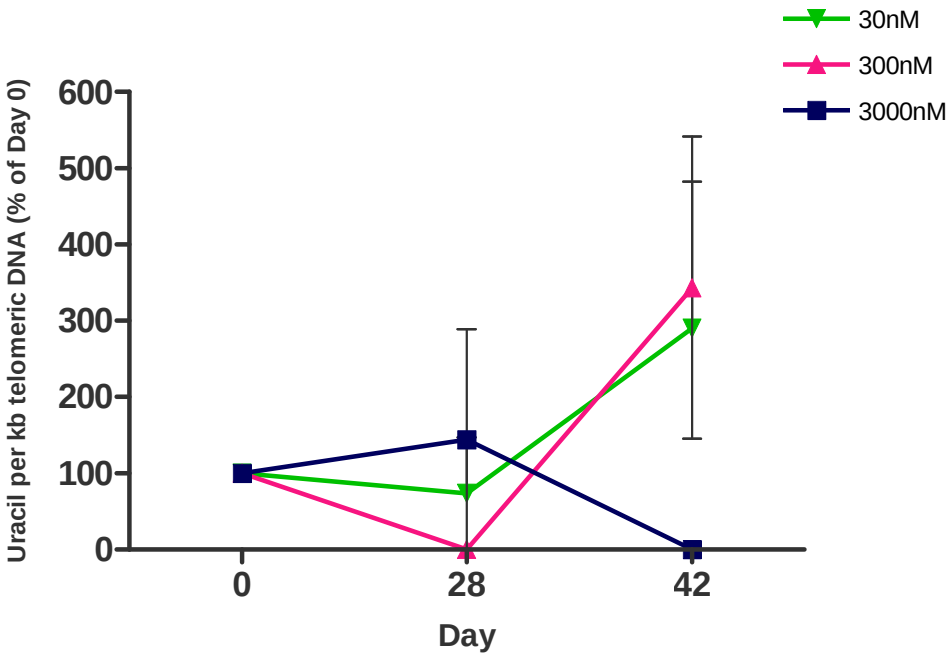

Source of variation	% of total variation	P value
Interaction	16.48	0.23
FA	2.34	0.65
Time	7.72	0.26

Figure 6.3 Uracil content in telomeric DNA of WIL2-NS cells grown in culture medium containing either 30, 300 or 3000nM FA for 42 days. Data is expressed as a percentage relative to the amount of uracil in telomeric DNA at day 0, with uracil in telomeric DNA at day 0 being set as 100%. (N = 4 for each data point. Error bars indicate SD. Data table represents the results of analysis by two-way ANOVA).

Table 6.1 Uracil content in telomeric DNA of WIL2-NS cells cultured in medium containing 30, 300 or 3000nM FA, and in medium containing 0, 0.2 or 1.0μM 5azadC. Uracil content in telomeric DNA of WIL2-NS cells cultured in medium containing (A) 30, 300 or 3000nM FA for 42 days; and (B) 0, 0.2 or 1.0μM 5azadC over 4 days. Data is expressed as a percentage relative to the amount of uracil in telomeric DNA at day 0; the latter was adjusted to 100%, and all other data calculated relative to this. (Data presented is mean ± SD. N = 4 for each value. P values represent results of analysis by two-way ANOVA).

(A) Uracil content of telomeric DNA in WIL2-NS cells cultured over 42 days in FA-deficient medium

	[FA] in medium (nM)			
Time	30	300	3000	
Day 0	100.0 ± 0.0	100.0 ± 0.0	100 ± 0.0	Effect of time p = 0.26
Day 28	73.6 ± 147.2	0.0 ± 0.0	144.5 ± 289.0	
Day 42	290.3 ± 384.1	343.4 ± 396.6	0.0 ± 0.0	
		Effect of FA, p = 0.65		Interaction, p = 0.23

(B) Uracil content of telomeric DNA in WIL2-NS cells cultured over 4 days in medium containing 5azadC

	[5azadC] in medium (μM)			
Time	0	0.2	1.0	
Day 0	100.0 ± 0.0	100.0 ± 0.0	100.0 ± 0.0	
Day 1	75.0 ± 50.2	87.6 ± 8.9	67.5 ± 22.3	Effect of time
Day 2	55.4 ± 38.8	50.0 ± 34.0	48.9 ± 19.6	p < 0.0001
Day 3	30.8 ± 40.7	24.2 ± 28.2	49.7 ± 28.7	
Day 4	58.1 ± 5.9	32.3 ± 34.6	0.0 ± 0.0	
		Effect of 5azadC, p = 0.45		Interaction, p = 0.22

6.3.3 Frequency of BN cells with multiple NPBs

The NPB data presented in Chapters 4 and 5 of this thesis shows (i) the frequency of binucleate (BN) WIL2-NS cells containing 1 or more NPB, and (ii) the total number of NPB present in 1000 BN cells, for each treatment at each time point, scored using the standard CBMN cytome assay scoring criteria.

The data presented in this chapter represents a re-scoring of all slides, with the purpose of expanding upon the NPB data presented in Chapters 4 and 5. For the 42-day FA study 1000 BN were re-scored per slide. For the 5azadC study, due to the low numbers of BN cells in the higher concentration condition, only 500 BN were re-scored per slide. For both studies, two slides were scored for each treatment, at each time point.

The data presented in this chapter represents the re-scoring of all slides to determine:

(i) the frequency of cells containing 1, 2, 3 or 4 NPB (based on standard scoring criteria) (Figure 6.4A-D);

(ii) the frequency of cells containing a number of NPB so high as to cause them to be indistinguishable as individual NPBs. The nuclear morphology of these cells is such that it resembles "chewing gum" between the two nuclei as they have attempted to separate at anaphase (Figure 6.4 E&F). Cells displaying 'chewing gum' morphology had not been included in the original data set for these experiments (Chapters 4 and 5) as they did not meet the standard scoring criteria for the CBMN Cytome assay (Chapter 3.3.6.6)[14].

(ii) the total number of NPB per 1000 BN for the FA study (per 500 BN for the 5azadC study), for each treatment at each time point. These data include "chewing gum" cells. Upon detailed re-scoring of the original slides, cells which displayed this morphology were identified and included in the data presented in this Chapter. To simplify the scoring protocol BN cells with 'chewing-gum' morphology were scored as having '5' NPB.

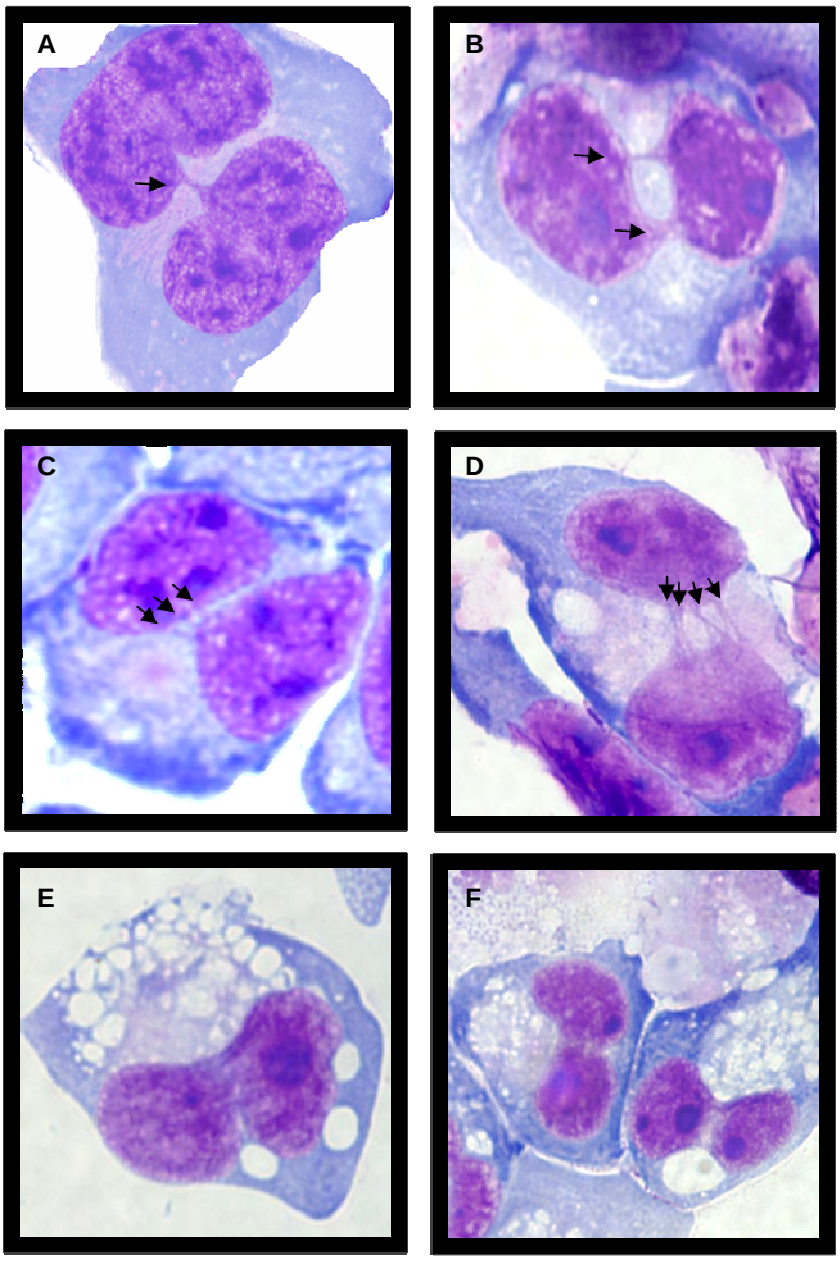

Figure 6.4 Representative photomicrographs of WIL2-NS cells with (A) 1, (B) 2, (C) 3 and (D) 4 NPBs, and (E & F) with nuclear morphology suggesting multiple NPBs ('chewing gum' morphologies; scored as '5' NPBs) (1000x magnification).

.

6.3.3.1 Long term (42 day) folic acid study

Significant differences were observed between the frequency of BN cells exhibiting 1 or 2 NPBs in WIL2-NS grown in medium containing 30, 300 or 3000nM FA, with a greater frequency observed in the lower FA treatments. Analysis by two-way ANOVA for the frequency of BN cells containing only 1 NPB showed that 55% of the variance was due to FA treatment ($p < 0.0001$) and 19.5% was due to the interaction of FA and time ($p = 0.002$) (Table 6.2A). 49.5% of the variance in BN cells exhibiting 2 NPB was explained by FA concentration in medium ($p < 0.0001$), and 28% by the interaction of FA with time ($p = 0.001$) (Table 6.2B).

The frequency of BN cells containing 3 or 4 NPBs was small for the majority of treatments and time points. These data sets were, therefore, combined and while actual frequencies remained low a significant difference was observed, with 25.2% of the variance being attributable to FA treatment ($p = 0.01$) (Table 6.2C).

The frequency of BN cells with 'chewing gum' morphologies cultured in 30nM FA over 42 days ranged from 1.5 ± 0.7 at day 0 to 39.5 ± 17.7 at day 35, followed by a small reduction to 30.5 ± 12 by day 42. The difference in frequencies between FA conditions was statistically significant with analysis by two-way ANOVA showing 36.5% of the variance was due to FA concentration in medium ($p < 0.0001$), 21.6% was due to time ($p = 0.0027$) and 29.7% was attributable to the interaction of both factors ($p = 0.006$) (Table 6.2D).

Comparison of the frequency of NPBs at day 42 by one-way ANOVA showed a significant difference between all conditions for BN with 1 NPB ($p = 0.004$) (Figure 6.5A), and BN with 2 NPB ($p = 0.01$) (Figure 6.5B). Trends for increasing frequencies of BN cells with 3 or 4, and '5' NPBs were observed in the lower FA concentrations at day 42, however, these did not reach statistical significance ($p = 0.6$ and 0.07, respectively) (Figure 6.5 C&D).

The total number of NPB per 1000 BN cells (including all clearly discernible NPBs as well as '5' NPB for each BN with 'chewing-gum' (CG) nuclear morphology), showed a strong increase in cells cultured in the lowest FA treatment. Analysis showed 46.8% of variance was attributable to FA concentration ($p < 0.0001$), 21.7% to time ($p < 0.0001$), while the interaction of FA with time explained 26.9% of the variance ($p < 0.0001$) (Figure 6.6A). Area under the

curve data obtained from this graph (AUC total NPBs (incl CG)) showed a significant, negative relationship with the concentration of FA in medium ($r = -0.92$, $p = 0.01$) (Figure 6.6B).

A positive correlation was observed between AUC TL (obtained from Figure 4.5) and AUC total NPB (incl CG), however, this did not achieve statistical significance ($r = 0.71$, $p = 0.1$) (Figure 6.6C). A significant, positive relationship was shown between the AUC total NPB (incl CG) and AUC LINE1 hypomethylation (obtained from Figure 6.1A) ($r = 0.97$, $p = 0.001$) (Figure 6.6D).

Table 6.2 The frequency of BN WIL2-NS cells displaying 1, 2, 3 or 4, or '5' NPB over 42 days in culture medium containing either 30, 300 or 3000nM FA. Data presented in (A) represents the frequency of cells, per 1000 BN, displaying (A) 1, (B) 2, (C) 3 or 4 clearly discernible NPB scored using standard CBMN Cyt scoring criteria. Data in Table D represents the frequency of BN cells displaying 'chewing gum' nuclear morphology which were scored as containing '5' NPB. (Mean ± SD is shown for each FA concentration at each time point. N = 2. P values represent analysis by two-way ANOVA. Data not sharing the same superscript letter within each time point differ significantly from each other, as measured by Bonferroni post test).

		[FA] in medium (nM)			
	Time	30	300	3000	
(A) BN cells with 1NPB	Day 0	11.5 ± 4.9	11.5 ± 4.9	11.5 ± 4.9	Effect of time p = 0.0002
	Day 14	49.5 ± 7.8	19.0 ± 7.1	11.0 ± 5.7	
	Day 28	59.5 ± 12.0[a]	18.0 ± 4.2[b]	5.0 ± 2.8[b]	
	Day 35	90.5 ± 30.4[a]	15.5 ± 6.4[b]	12.5 ± 3.5[b]	
	Day 42	83.0 ± 7.1[a]	29.5 ± 3.5[b]	26.0 ± 7.1[b]	
		Effect of FA, p < 0.0001			Interaction, p = 0.0021
(B) BN cells with 2 NPB	Day 0	1.0 ± 0.0	1.0 ± 0.0	1.0 ± 0.0	Effect of time p = 0.0037
	Day 14	2.0 ± 0.0	0.0 ± 0.0	0.0 ± 0.0	
	Day 28	4.0 ± 1.4[a]	0.5 ± 0.7[b]	0.5 ± 0.7[b]	
	Day 35	4.5 ± 2.1[a]	1.5 ± 0.7[b]	0.5 ± 0.7[b]	
	Day 42	8.0 ± 1.4a	1.0 ± 1.4[b]	0.0 ± 0.0[b]	
		Effect of FA, p < 0.0001			Interaction, p = 0.0012
(C) BN cells with 3 or 4 NPB	Day 0	0.0 ± 0.0	0.0 ± 0.0	0.0 ± 0.0	Effect of time p = 0.1612
	Day 14	1.5 ± 0.7	0.5 ± 0.7	0.0 ± 0.0	
	Day 28	0.0 ± 0.0	0.0 ± 0.0	0.0 ± 0.0	
	Day 35	2.0 ± 1.4	0.0 ± 0.0	0.0 ± 0.0	
	Day 42	1.0 ± 1.4	0.0 ± 0.0	0.0 ± 0.0	
		Effect of FA, p = 0.0135			Interaction, p = 0.2373
(D) BN cells with '5' NPB	Day 0	1.5 ± 0.7	1.5 ± 0.7	1.5 ± 0.7	Effect of time p = 0.0027
	Day 14	7.5 ± 2.1	4.5 ± 0.7	2.5 ± 0.7	
	Day 28	13.0 ± 5.7	3.5 ± 0.7	1.0 ± 0.0	
	Day 35	39.5 ± 17.7[a]	3.0 ± 1.4[b]	2.0 ± 1.4[b]	
	Day 42	30.5 ± 12.0[a]	6.5 ± 0.7[b]	7.5 ± 2.1[b]	
		Effect of FA, p < 0.0001			Interaction, p = 0.0055

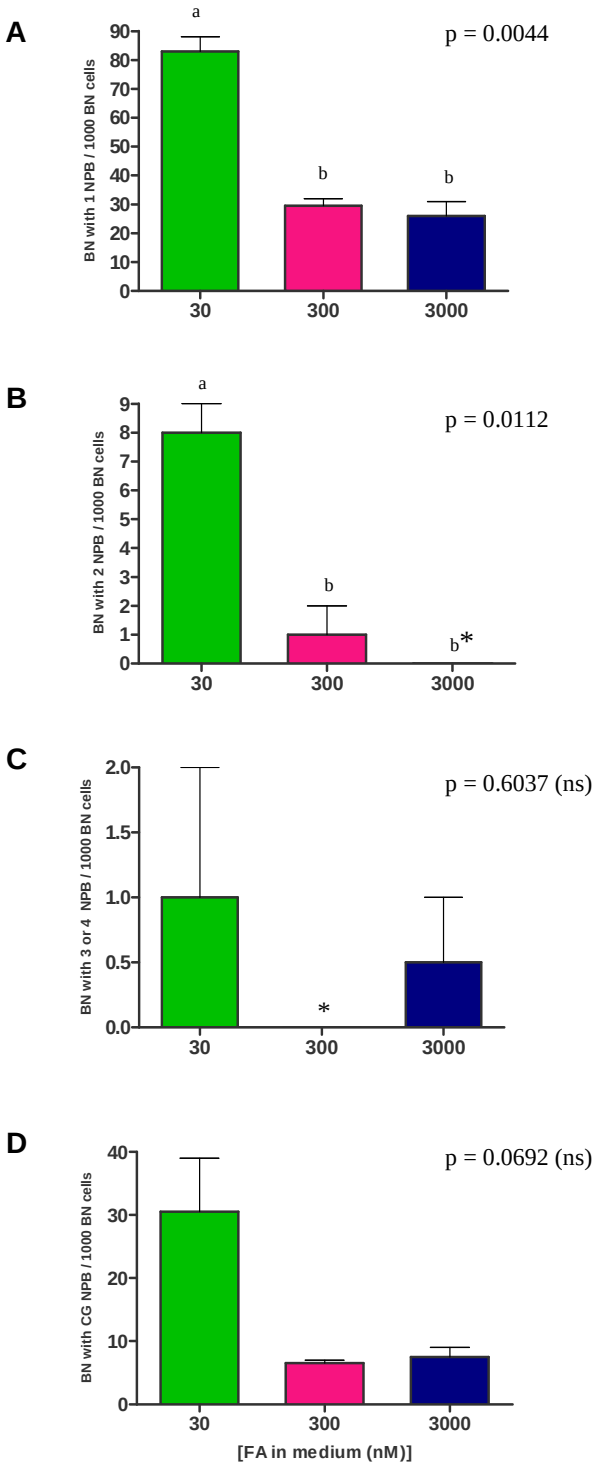

Figure 6.5 The frequency per 1000 BN cells which contain 1, 2, 3 or 4, and '5' NPB following 42 days in culture medium containing either 30, 300 or 3000nM FA. Frequency of BN cells containing (A) 1, (B) 2, (C) 3 or 4 clearly discernible NPB scored using standard CBMN Cyt scoring criteria. Data in Figure D represents the frequency of BN cells displaying 'chewing gum' nuclear morphology which were scored as containing '5' NPB. N = 2. Error bars indicate SD. P values reflect analysis by one-way ANOVA at day 42. Columns not sharing the same letter are significantly different from each other, as measured by Tukey's post test. (ns; not statistically significant. * No BN cells recorded for this category).

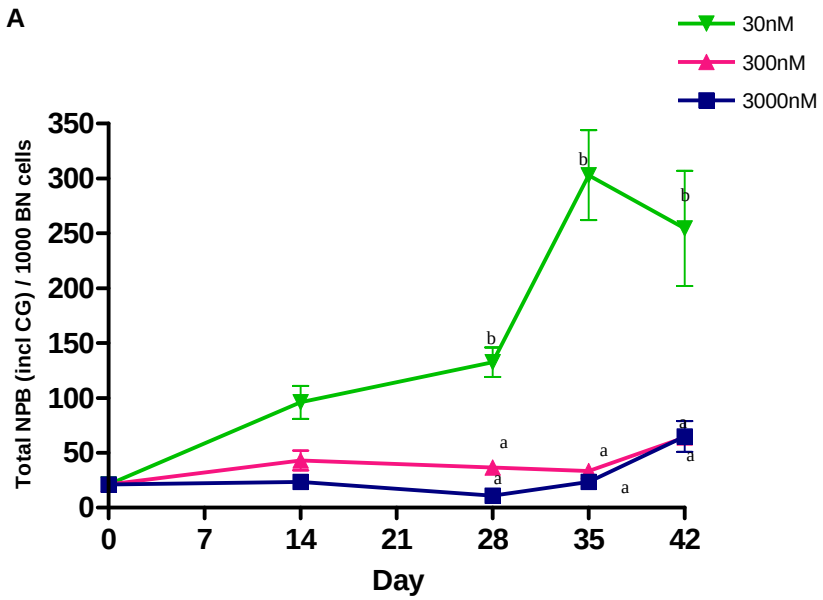

Source of variation	% of total variation	P value
Interaction	26.89	<0.0001
FA	46.81	<0.0001
Time	21.70	<0.0001

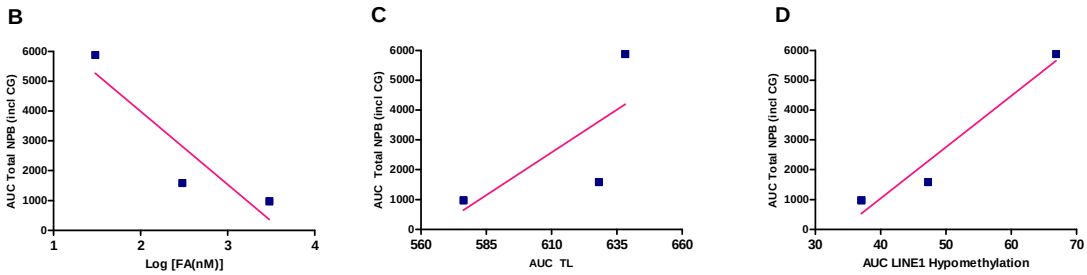

Figure 6.6 The total number of NPB per 1000 BN WIL2-NS cells cultured over 42 days in medium containing either 30, 300 or 3000nM FA. (A) The total number of NPBs per 1000 BN cells, including NPB scored using standard criteria for the CBMN Cytome assay, as well as BN cell displaying 'chewing gum' (CG) nuclear morphology which were scored as containing '5' NPB each. (Data table represents results of analysis by two-way ANOVA. N = 2. Error bars indicate SD. Points not sharing the same letter at each time point differ significantly from each other, as measured by Bonferroni post test). Relationships between AUC total NPB (incl CG) with (B) FA concentration in culture medium, (C) AUC TL, and (D) AUC LINE1 hypomethylation.

6.3.3.2 5azadC study

Significantly higher frequencies of BN WIL2-NS (per 500 BN cells) containing 1 or 2 NPBs were observed in cells grown in medium containing 0.2 and 1.0µM 5azadC, compared to those cultured in 0µM. Analysis by two-way ANOVA for the frequency of BN cells with only 1 NPB showed 25.9% of the variance was due to 5azadC treatment ($p < 0.0001$), 48.3% was due to time ($p < 0.0001$), and 23.8% of variance was attributable to the interaction of both factors ($p < 0.0001$) (Table 6.3A). 30.7% of the variance in cells exhibiting 2 NPB was attributable to 5azadC treatment ($p < 0.0001$) and 24.6% to the interaction of treatment with time ($p = 0.005$) (Table 6.3B).

The frequency of BN cells with 3 or with 4 NPBs was again negligible for the majority of treatments and time points. These data sets were combined, and significant differences were observed between treatments, with 18.3% of the variance being attributable to 5azadC treatment ($p = 0.006$). The interaction of treatment with time explained 24.5% of variance, but was not statistically significant ($p = 0.06$) (Table 6.3C).

The frequency of BN cells meeting the criteria for 'chewing gum' morphologies increased from 4.5 ± 3.5 at day 0 to 160 ± 93.3 after 4 days in the highest (1.0µM) 5azadC treatment. The difference in frequencies was statistically significant with 23.8% of the variance attributable to 5azadC concentration in medium ($p = 0.001$) and 40.2% due to time ($p = 0.0005$). Interaction of treatment with time was responsible for 20.06% of variance, however, this was not significant ($p = 0.07$) (Table 6.3D).

Comparison of the frequency of NPBs at day 4 by one-way ANOVA showed a significant difference between all conditions for BN with 1 NPB ($p = 0.004$) (Figure 6.7A), while the difference in BN cells with 2 NPB was not significant ($p = 0.055$) (Figure 6.7B). Trends for increasing frequencies of BN cells with 3 or 4, and '5' NPBs were observed in the higher concentration treatments at day 4, however, these did not reach statistical significance ($p = 0.27$ and 0.24, respectively) (Figure 6.7 C&D).

The total number of NPB (including '5' NPB for each BN with 'chewing-gum' nuclear morphology) showed a strong increase in cells cultured in the highest 5azadC treatment. Analysis showed 25.2% of variance was attributable to 5azadC concentration ($p = 0.0002$),

42.2% to time ($p < 0.0001$), while the interaction of treatment and time explained 21.3% of the variance ($p = 0.02$) (Figure 6.8A).

Significant, positive correlations were observed between area under the curve obtained from Figure 6.8A (AUC total NPB (incl CG)) and the concentration of 5azadC in culture medium ($r = 0.88$, $p = 0.02$) (Figure 6.8B), as well as between AUC total NPB (incl CG) and AUC TL ($r = 0.86$, $p = 0.03$) (Figure 6.8C). A significant, positive relationship was also observed between AUC total NPB (incl CG) and AUC LINE1 hypomethylation ($r = 0.91$, $p = 0.01$) (Figure 6.8D).

TABLE 6.3 The frequency of BN WIL2-NS cells displaying 1, 2, 3 or 4, or '5' NPB following culture in complete medium containing either 0, 0.2 or 1.0μM 5azadC over 4 days. Data presented in Tables A-C represents the frequency of cells, per 500 BN cells, displaying (A) 1, (B) 2, and (C) 3 or 4 NPB scored using standard CBMN Cyt scoring criteria. Data in Table D represents the frequency of BN cells displaying 'chewing gum' nuclear morphology which were scored as containing '5' NPB. (Mean ± SD is shown for each 5azadC concentration at each time point. N = 2. P values represent analysis by two-way ANOVA. Data not sharing the same superscript letter within each time point differ significantly from each other, as measured by Bonferroni post test).

		[5azadC] in medium (μmol/L)			
	Time	0	0.2	1.0	
(A) BN cells with 1 NPB	Day 0	7.5 ± 2.1	7.5 ± 2.1	7.5 ± 2.1	Effect of time p < 0.0001
	Day 1	8.0 ± 1.4	17.0 ± 4.2	8.5 ± 0.7	
	Day 2	11.5 ± 3.5^{b}	17.0 ± 5.7^{b}	40.0 ± 8.5^{a}	
	Day 3	10.5 ± 3.5^{c}	57.5 ± 4.9^{b}	74.5 ± 10.6^{a}	
	Day 4	14.5 ± 9.2^{c}	58.5 ± 7.8^{b}	88.5 ± 0.7^{a}	
		Effect of 5azadC, p < 0.0001			Interaction, p < 0.0001
(B) BN cells with 2 NPB	Day 0	1.0 ± 0.0	1.0 ± 0.0	1.0 ± 0.0	Effect of time p < 0.0001
	Day 1	1.0 ± 1.4	1.0 ± 1.4	0.5 ± 0.7	
	Day 2	1.0 ± 0.0^{b}	3.5 ± 3.^{5ab}	12.0 ± 4.2^{a}	
	Day 3	0.0 ± 0.0^{b}	9.0 ± 2.8^{a}	17.5 ± 6.4^{a}	
	Day 4	1.5 ± 0.7^{b}	11.0 ± 2.8^{a}	18.5 ± 6.4^{a}	
		Effect of 5azadC, p < 0.0001			Interaction, p = 0.0054
(C) BN cells with 3 or 4 NPB	Day 0	0.0 ± 0.0	0.0 ± 0.0	0.0 ± 0.0	Effect of time p = 0.0012
	Day 1	1.0 ± 1.4	1.5 ± 2.1	0.0 ± 0.0	
	Day 2	0.5 ± 0.7	1.0 ± 0.0	2.5 ± 0.7	
	Day 3	0.5 ± 0.7^{b}	6.5 ± 0.7^{ab}	9.5 ± 3.5^{a}	
	Day 4	0.5 ± 0.7^{b}	5.5 ± 4.9^{ab}	10.0 ± 5.7^{a}	
		Effect of 5azadC, p = 0.0057			Interaction, p = 0.0608 (ns)
(D) BN cells with '5' NPB*	Day 0	4.5 ± 3.5	4.5 ± 3.5	4.5 ± 3.5	Effect of time p = 0.0005
	Day 1	4.5 ± 2.1	9.5 ± 4.9	11.0 ± 1.4	
	Day 2	2.5 ± 2.1	22.5 ± 20.5	70.0 ± 1.4	
	Day 3	7.0 ± 5.7^{b}	104.5 ± 0.7^{a}	117.5 ± 10.6^{a}	
	Day 4	11.0 ± 8.5^{b}	109.5 ± 77.1^{a}	160.0 ± 93.3^{a}	
		Effect of 5azadC, p = 0.001			Interaction, p = 0.07 (ns)

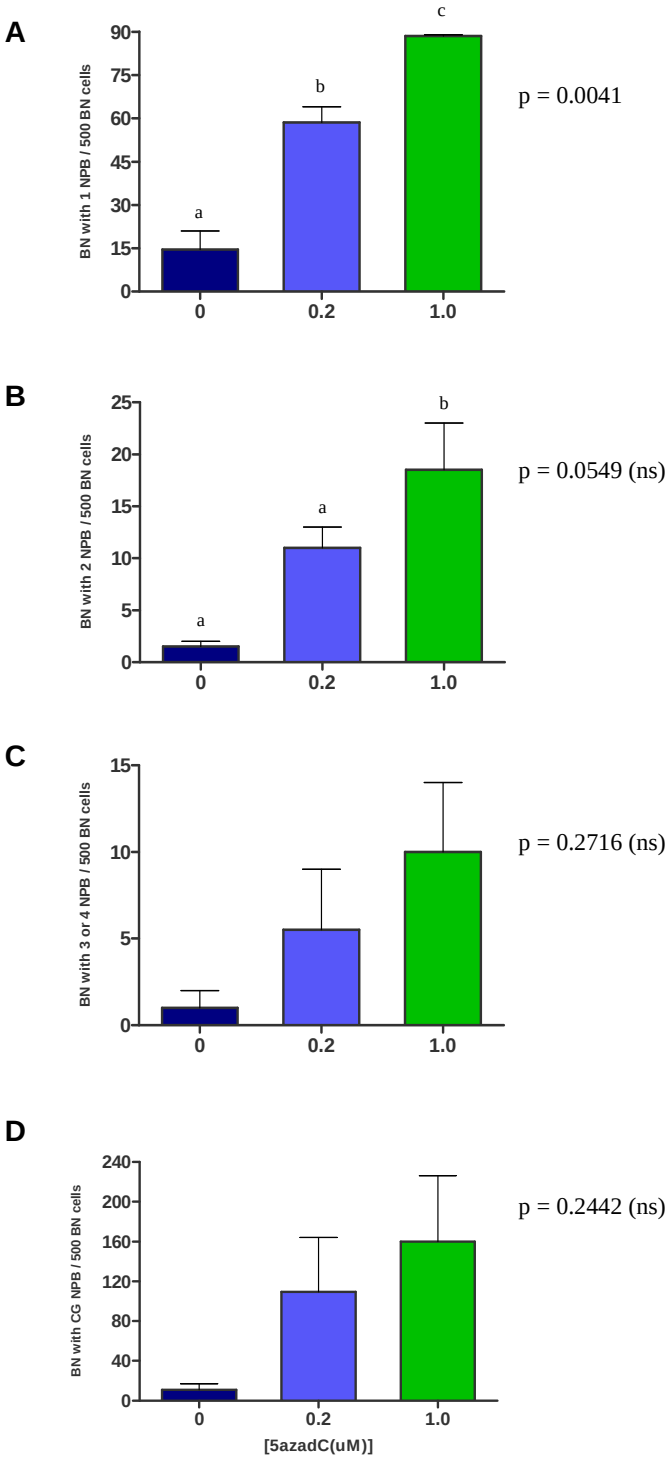

Figure 6.7 The frequency of cells, per 500 BN WIL2-NS cells, containing 1, 2, 3 or 4, and '5' NPB following 4 days culture in medium containing either 0, 0.2 or 1.0μM 5azadC. Data presented in Figures A-C represents the frequency of cells at day 4, per 500 BN cells, displaying (A) 1, (B) 2, and (C) 3 or 4 NPB scored using standard CBMN Cyt scoring criteria. Data in Figure D represents the frequency of BN cells displaying 'chewing gum' (CG) nuclear morphology which were scored as containing '5' NPB. (N = 2. Error bars indicate SD. P values reflect analysis by one-way ANOVA at day 42. Columns not sharing the same letter are significantly different from each other, as measured by Tukey's post test. ns; not statistically significant).

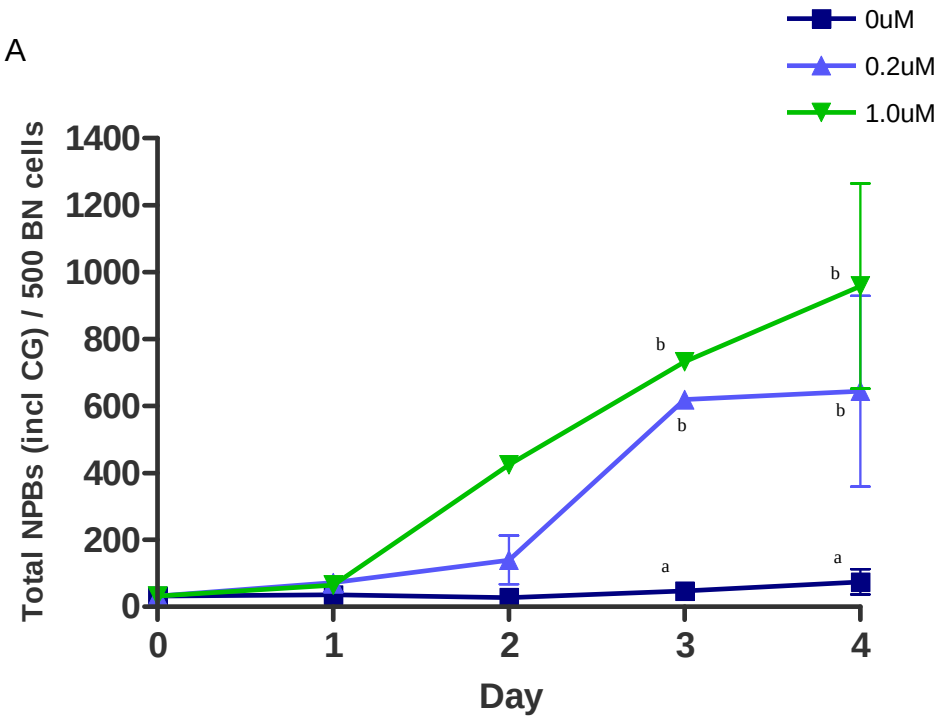

Source of variation	% of total variation	P value
Interaction	21.29	0.0170
5azadC	25.16	0.0002
Time	42.23	< 0.0001

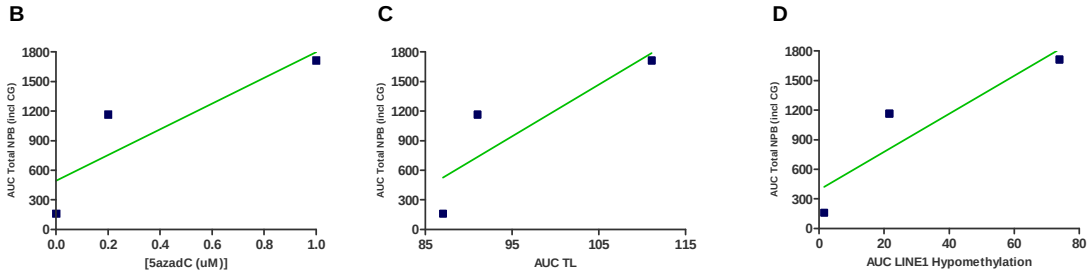

r = 0.8765
p = 0.0219

r = 0.8588
p = 0.0285

r = 0.9128
p = 0.0111

Figure 6.8 The total number of NPB per 500 BN WIL2-NS cells cultured in medium containing either 0, 0.2 or 1.0μM 5azadC over 4 days. (A) The total number of NPB per 500 BN cells including individual NPB scored using standard criteria for the CBMN Cytome assay, as well as BN cells displaying 'chewing gum' (CG) nuclear morphology which were scored as containing '5' NPB each. (Data table represents results of analysis by two-way ANOVA. N = 2. Error bars indicate SD. Points not sharing the same letter at each time point differ significantly from each other, as measured by Bonferroni post test). Relationships between AUC total NPB (incl CG) and (B) 5azadC concentration in culture medium, (C) AUC TL, and (D) AUC LINE1 hypomethylation.

6.4 DISCUSSION

6.4.1 Global (LINE1) DNA Methylation Status

The global DNA methylation status of LINE1 repeating sequences was used in this study to provide an indirect measure of subtelomeric methylation. Over the course of the 42-day FA study, the degree of LINE1 hypomethylation increased significantly in the lower FA treatments, in a dose-dependent manner. These data are in agreement with the hypothesis that cells cultured in 30 and 300nM FA would have reduced levels of LINE1 methylation, when compared with the FA-replete (3000nM) treatment. The relationship observed between FA concentration and hypomethylation was significant and negative, also in agreement with previous reports[360-363]. It is possible, however, that the effect of FA deficiency on methylation may differ in short and long term cultures causing a differential effect on TL.

In the 5azadC study a rapid, significant increase in hypomethylation of LINE1 was recorded in the 1.0 and 0.2µM conditions. A highly significant, positive association was observed between LINE1 hypomethylation and the concentration of 5azadC in culture medium. This observation is consistent with previous reports[319,356], and supports the proposed hypothesis that hypomethylation would be observed in WIL2-NS treated in 0.2 and 1.0µM 5azadC culture over four days.

Interestingly, the relationship between LINE1 hypomethylation and telomere length was found to be significant and positive in the FA study. This effect was also observed in the 5azadC study where the rapid impact of DNMT inhibition showed increasing TL as global methylation levels reduced. The correlation between hypomethylation by 5azadC with telomere elongation is in agreement with the findings of Vera *et al* (2008) who tested TL and hypomethylation using 5azadC in a panel of human cancer cell lines[319]. The telomere elongating effect of hypomethylation arising from FA insufficiency has not, however, been reported previously.

Hypomethylation was also positively, and significantly, associated with increasing levels of chromosome damage biomarkers in both the FA and the 5azadC studies. Previous reports have shown that reduced FA[35,56,93] and increased 5azadC[356] result in increased levels of DNA damage. Given hypomethylation, both globally and specifically at the subtelomere, has been associated with increased levels of recombination and sister chromatid exchange (SCE), it is plausible that increased CIN and damage are generated by this effect. Accordingly, whether the mechanistic link between hypomethylation and increased CIN is coincident or causal requires further investigation, and this is discussed in greater detail below in 6.4.3.3.

6.4.2 Uracil incorporation into telomeres

The incorporation of uracil into genomic DNA where thymidylate stress occurs from folate-insufficiency is well documented[74,91,92,98,99,364,365]. The original hypothesis proposed for this study was that, due to the high thymidine content, telomeric DNA would be particularly vulnerable to uracil incorporation under low folate conditions. In support of this hypothesis, experimental findings presented in Chapter 4 of this thesis showed a rapid decrease in TL in cells in the lowest FA treatment from day 14-42 of the long term FA study. Mechanistically, it is proposed that the telomere shortening may have been due to double strand breakage arising from uracil incorporation into DNA, followed by the subsequent action of uracil glycosylase and APE1 endonuclease as part of the BER pathway, resulting in abasic sites and transient strand breaks in DNA[74,75,92,100,365].

It is interesting to note that the generation of DSBs by the uracil glycosylase pathway, while potentially deleterious in the context of telomere biology, forms a key component of a functional immune response in B cells[366,367]. In this context cytosine residues in the immunoglobulin gene locus are enzymatically deaminated to uracil, generating an abasic site by uracil glycosylase cleavage[366]. These abasic sites are then converted to SSBs by APE1 and APE2. Where SSBs occur in close proximity on opposite strands double strand breakage results, thus facilitating the recombination events required for immunoglobulin class switching[366,367]. The effectiveness of this mechanism to generate DSBs where required for class switching demonstrates the potential for negative effects of high uracil content in other areas of the genome, including in the telomere. This may be of particular relevance in the WIL2-NS, a B lymphoblastoid cell line.

Results presented in this chapter, obtained using a novel quantitative realtime PCR (qPCR) method to measure the degree of incorporation of uracil into telomeric DNA sequences, were not statistically significant. A clear trend was observed, however, with increased uracil in the telomeres of cells in the lower FA treatments (30 and 300nM) after 42 days in culture, compared to the FA-replete control (3000nM). No increase in uracil was recorded in cells cultured for 42 days in FA replete medium.

Slightly more uracil was recorded in the mid-range (300nM) FA treatment at day 42, compared to the lowest (30nM) FA concentration. This result is consistent with the effect observed by Mashiyama *et al*, who demonstrated that as FA concentration in medium increased, the rate of cell division decreased, thus the capacity for uracil incorporation into newly synthesised DNA was reduced[99]. Cells in medium containing a higher (yet still deficient) concentration of FA

continued to divide at a steady rate, thus greater uracil incorporation was observed in these cells[99]. Nuclear division index (NDI) data presented in Figure 4.3D of this thesis indicates that this effect was observed in the 42-day FA study, whereby NDI for cells in the mid-range (300nM) culture was relatively constant, ranging from 1.37 ± 0.05 at day 14 to 1.07 ± 0.05 at day 42. NDI of cells in the 30nM treatment, on the other hand, reduced significantly and rapidly from 1.34 ± 0.18 at day 0 to 0.79 ± 0.01 at day 14, and 0.07 ± 0.25 at day 42. The differences in NDI due to the effect of FA treatment, time and their interaction were highly significant. Accordingly, it is plausible that the amount of uracil observed in the cells cultured in 300nM FA for 42 days is greater than that of cells in 30nM FA due to the greater proportion of cells undergoing DNA synthesis and, therefore, incorporating uracil into DNA.

As predicted, and consistent with previous studies on genomic DNA, an inverse correlation was observed between uracil in the telomere at day 42 and FA concentration in medium. Also as hypothesised, but not previously reported, a non-significant, inverse relationship was apparent between the presence of uracil in the telomere and telomere length after 42 days in culture. This evidence is preliminary and will require further studies to consolidate and verify the observations made.

The hypothesis that uracil content would remain unchanged in the telomeres of cells cultured in 0, 0.2 or 1.0µM 5azadC was supported by the results of the present study. The rationale for this hypothesis was that 5azadC impacts on DNA methylation via inhibition of DNMT activity, while having no reported impact on dTTP availability, or the conversion of dUTP to dTTP. Analysis showed that 5azadC had no impact on the amount of uracil in telomeric sequences. It is possible that the lack of effect may be due, in part, to the short time frame (4 days) for this study, however, statistically significant increases in uracil content in genomic DNA has been reported after as few as 8-10 days in culture under low FA conditions[91,98,99].

It should be noted that the method used for the uracil analysis has not yet been fully optimised and continues to be refined. One component that is believed may increase assay sensitivity is the addition of an endonuclease following the digestion step, and this is currently being tested. It should also be noted that this qPCR method is an indirect measure of uracil within telomeric DNA and does not differentiate between: (i) uracil incorporation due to thymidylate stress (observed under low folate conditions)[365]; or (ii) uracil arising from the spontaneous deamination of cytosine residues[97]. The latter pathway leads to pro-mutagenic U:G mismatching[97], and may subsequently lead to single base mutations in the genomes of daughter cells. As such, the results presented here should be viewed as preliminary.

In summary, uracil in telomeric DNA sequences increased in WIL2-NS cells cultured in medium containing 30 and 300nM FA, while remaining unchanged in cells in FA-replete (3000nM) medium. Uracil in telomeric DNA was unchanged by treatment with 5azadC, suggesting that the 'chewing gum' morphologies may be due to reduced DNMT action, and not uracil-induced chromosome breakage.

6.4.3 Frequency of nucleoplasmic bridges (NPBs)

The frequencies of BN cells displaying 1, 2, 3/4 (combined), or '5' NPB all differed significantly between concentrations of FA or 5azadC in medium, with higher numbers observed in cells grown in low FA, and in high 5azadC conditions. It is interesting to note the very low frequencies of BN cells recorded as having 3 or 4 NPB, given the very high numbers of cells which were then recorded with 1 or 2, and with very high numbers (CG cells) in the same populations. This may be due to a compounding effect, whereby cells with one or two NPB remain viable over several population doublings, whereas cells with multiple chromosome fusions may be expected to degenerate more rapidly, through BFB cycling, and may develop CG morphology, and/or become non-viable.

The frequency of BN WIL2-NS cells displaying multiple ('5') NPB, resulting in the 'chewing gum (CG)'-like morphology, increased significantly from day 0 to day 42 in cells grown in low FA, peaking at 30 ± 12 per 1000 BN at day 35. These frequencies were low, however, relative to those observed after only four days in medium containing 1.0µM 5azadC, for which more than 5-fold this frequency (160 ± 93 per 1000 BN) was observed.

The total number of NPB (including CG cells which were counted as having '5' NPB each) increased significantly in the 30nM FA treatment over the course of the 42 day FA study. The maximum number of NPB observed was 303 ± 58 per 1000 BN at day 35 in the low (30nM) FA treatment. Consistent with data presented in Chapter 4 (Tables 4.7 and 4.8), total NPB (including CG cells) correlated significantly and positively with telomere length, and negatively with FA concentration in medium. The total number of NPBs, also increased significantly in cells cultured in 0.2 and 1.0µM 5azadC over 4 days. The maximum frequency of NPB observed was 959 ± 433 per 1000 BN in the 1.0µM treatment at day 4. Large SD values for this category of NPB are evident in the latter stages of the studies when the cells are at their most damaged, suggesting that some refinement of scoring criteria for these morphologies may be required in future studies where high levels of damage are observed (examples in Figure 4.12 showing representative photomicrographs of cells at day 35 and 42 of

the long term FA dose response study). Interestingly, in both the FA study, and the 5azadC study, highly significant, positive correlations were observed between the total number of NPBs and global hypomethylation.

The origins of NPBs are many and varied. For example telomere end fusions due to dysfunctional TRF2 appear to be NHEJ dependent and involve large sequences of telomeric DNA[172]. In contrast, fusions between short telomeres have been observed in the absence of NHEJ factors[263], and data from human lymphocytes suggests that NPBs may also arise from assymetrical rearrangements of homologous or non-homologous chromosomes due to misrepair of DNA breaks[30]. Ultrafine bridges have been shown to occur where BLM protein is dysfunctional (Bloom syndrome)[368], and NPBs are evident in Werner syndrome where a mutation in the WRN helicase leads to accelerated telomere shortening[240]. Defects in the separation of sister chromatids at telomeres have also been shown to cause NPBs between daughter nuclei with intact telomeres[322]. Depending on the stage in the cell cycle at which they occur, DSBs and/or deletion events can lead to the formation of dicentric chromosomes, ring chromosomes and/or acentric fragments[30,125,276,279]. Following replication and nuclear envelope formation, these aberrations can be visualised as NPBs (dicentric chromosomes) and MNi (acentric fragments)[30]. It has been reported that breakage of NPBs can occur at multiple sites, potentially leading to extensive losses of genetic material[277]. While the implications of chromosome fusions are well documented, most notably in neoplastic cells exhibiting high levels of structural and numerical chromosome aberrations[277], the underlying mechanistic basis for fusions occurring between dysfunctional or critically shortened telomeres in humans remains unclear[125].

Four plausible mechanisms, acting separately or in concert, may underlie the dramatic increase in NPBs observed in the experiments reported in this thesis. These are summarised here, presented diagrammatically in Figure 6.9 below, and discussed in greater detail in the following pages:

1. Under folate limiting conditions, the presence of uracil, and/or intermediates arising from BER processes to remove and replace uracil, may disrupt binding of telomere capping proteins, leading to compromised telomere integrity and increased fusigenic potential of intact telomeres.
2. Under folate limiting conditions, abasic sites generated by BER mechanisms recruited to replace uracil in the telomere may increase the likelihood of single and double strand breaks (SSB and DSBs). Treatment with 5azadC is also reported to cause single and DSBs. Breakage may cause accelerated telomere shortening resulting in compromised

chromosome ends, and increased fusigenic potential of shortened telomeres. Single strand breaks are also associated with telomere-damaged induced foci (TIFs) whereby repair mechanisms are recruited, potentially leading to misrepair and dicentric chromosome formation.

3. Subtelomeric hypomethylation arising from (i) reduced availability of methyl groups via S-adenosyl methionine (SAM) (under folate limiting conditions), or (ii) direct inhibition of DNMT enzyme activity, may result in increased homologous recombination (HR) and/or increased sister chromatid exchanges involving telomeres (T-SCE). These mechanisms may potentially lead to fusions between uncapped chromosomes, dicentric chromosome formation, BFB cycling and rapid changes in telomere content in cells.
4. A tankyrase 1 (Tank1) knockdown model has shown multiple NPBs at anaphase arising from telomere fusions between sister chromatids[322]. Separation of chromatids at telomeres is effected by Tank1 in concert with TRF1 and cohesins[369]. The global hypomethylating effects of both low FA and 5azadC treatment may impact this pathway leading to dysfunctional separation at anaphase, and bridge formation.

All of these mechanisms potentially result in chromosome breakage, NPBs and BFB cycling. A proposed model as to how BFB cycling may lead to increased telomere content is presented graphically at Figure 6.9.

Figure 6.9 (Following page) Proposed pathways for generation of nucleoplasmic bridges (NPBs) in WIL2-NS cultured in low folic acid or in the presence of 5azadC. (TRF1/2, telomere repeat binding factor 1 and 2; TIF, telomere-damaged induced foci; BER, base excision repair; SAM, S-adenosyl methionine; DNMT, DNA methyltransferase; T-SCE, sister chromatid exchange involving telomeres; Tank1, tankyrase 1; TIN2, TRF1-interacting protein 2; BFB, breakage, fusion, bridge).

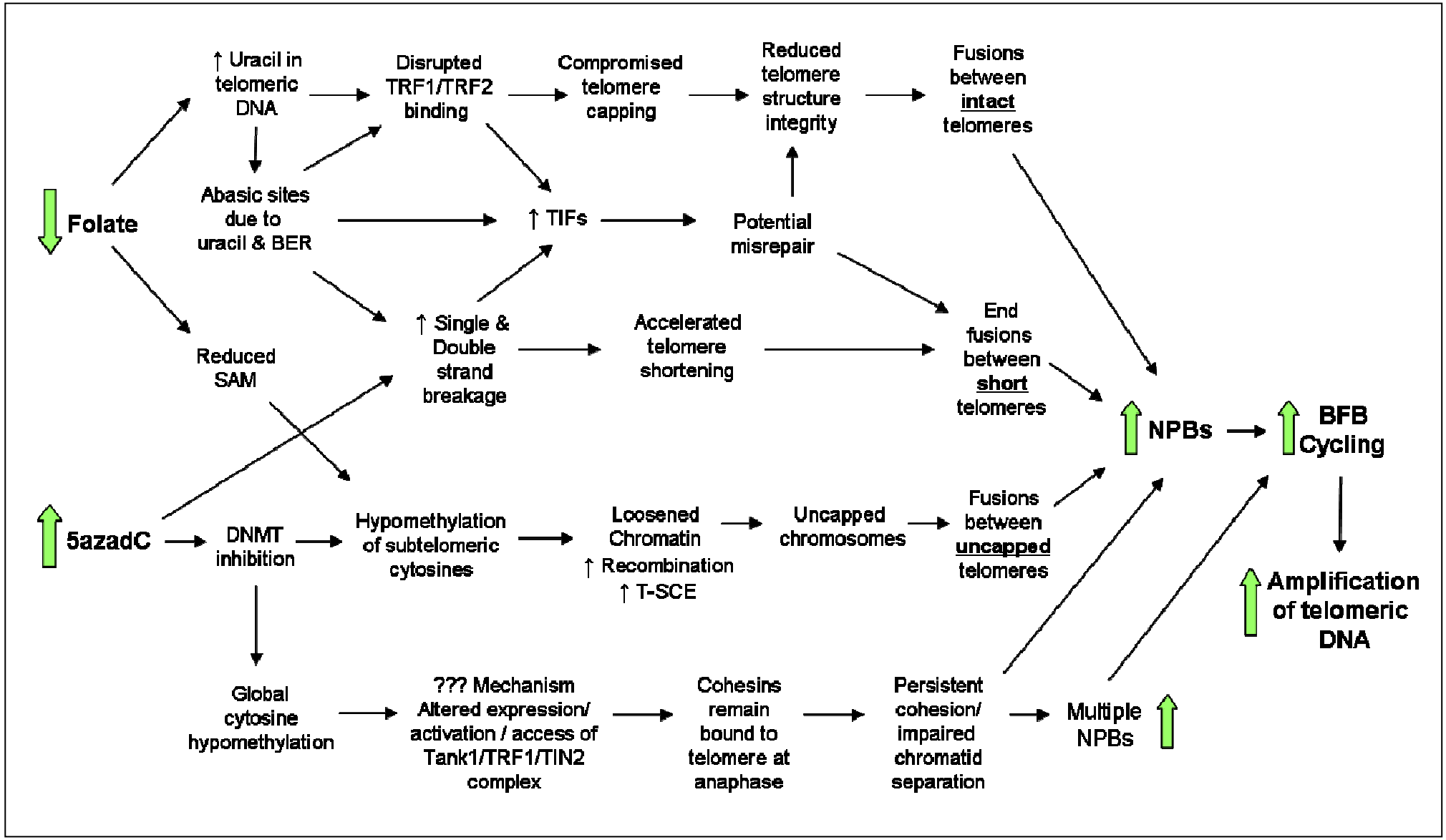
↑ Uracil in telomeric DNA
Disrupted TRF1/TRF2 binding
Compromised telomere capping
Reduced telomere structure integrity
Fusions between intact telomeres
Folate
Abasic sites due to uracil & BER
↑ TIFs
Potential misrepair
↑ Single & Double strand breakage
Accelerated telomere shortening
End fusions between short telomeres
Reduced SAM
NPBs
BFB Cycling
5azadC
DNMT inhibition
Hypomethylation of subtelomeric cytosines
Loosened Chromatin
↑ Recombination
↑ T-SCE
Uncapped chromosomes
Fusions between uncapped telomeres
Amplification of telomeric DNA
Global cytosine hypomethylation
??? Mechanism
Altered expression/ activation / access of Tank1/TRF1/TIN2 complex
Cohesins remain bound to telomere at anaphase
Persistent cohesion/ impaired chromatid separation
Multiple NPBs

6.4.3.1 Altered chromatin & compromised capping may lead to fusions of intact telomeres

Short telomeres had previously been thought to be the key initiating factor for chromosome end fusions, however a study exploring the fusigenic potential of different chromosome arms demonstrated that this was not always the case[329]. Slijepcevic *et al* (1997) explored the fusigenic potential of long and short telomeres in a mammalian cell line model and found that short telomeres did not correlate with increased incidence of fusions, and that long telomeres were in fact the more fusigenic[329]. Due to the presence of chromatin strands between linked telomeres, and evidence of fusions in conditions characterised by defective chromatin structure, these authors speculated that fusions between intact telomeres may be determined by chromatin status[329].

Effective telomere capping, specifically by TRF1 and TRF2, has also been shown to be critical for maintaining telomere integrity, and to prevent end fusions[153,172]. Experimental models using mammalian cells with disrupted TRF2 binding showed telomere end deprotection, cleavage of the 3' telomere overhang and end-to-end chromosome fusions by the non-homologous end joining (NHEJ) pathway[172,199,370-372]. Both TRF1 and TRF2 inhibition have been shown to cause telomeres to co-localise with DNA DSB response and repair factors, including activated ATM and the MRN complex[153,199,249], as well as instigating the phosphorylation of H2AX to γH2AX, indicative of TIFs[153,199,249,257]. These findings strongly suggest that reduced TRF1 and TRF2 binding leads to uncapped telomeres which are recognised by the cellular machinery as being a DSB requiring repair, resulting in NHEJ[199]. Interestingly, the end-to-end fusions observed by van Steensel *et al* (1998) in a dominant negative TRF2 model occurred from the loss of the 3' G-tail, while the telomeric sequence remained intact[172]. The findings of Martinez *et al* (2009) in a mouse model suggested that TRF1-depleted telomeres are prone to breakage, leading to chromosome fusions[153]. These authors propose that dysfunctional TRF1 binding is sufficient to produce severe telomeric damage, and potentially neoplastic changes, in the absence of telomere shortening as the initiating factor[153].

Capping proteins TRF1 and TRF2 are highly sensitive to conformational changes in their binding sites within the telomere[139]. Opresko *et al* demonstrated that the physical disruption of capping protein binding sites with oxidised guanine lesions (8-oxo-guanine) rapidly and significantly inhibited TRF1 and TRF2 binding[139]. Further to this, these researchers showed that BER intermediates, such as abasic sites or single nucleotide gaps, had a similarly disruptive impact on TRF1/2 binding kinetics[139]. In the present study, increased numbers of NPBs were observed in the cells with the highest concentrations of uracil present in telomeric

DNA. Accordingly, it is plausible that (i) the presence of uracil in the telomere sequence may have a similarly disruptive effect on TRF1/2 binding to that of 8-oxo-guanine, and (ii) intermediates of BER recruited to excise and replace uracil may also result in reduced binding affinity of these critical capping proteins. Thus, it is proposed that uracil incorporation into telomeric DNA, when folate is limiting, may have caused chromosome ends to become more fusigenic via both these mechanisms acting in concert, resulting in the increased numbers of NPB observed in the FA studies.

Together these findings suggest that the presence of telomeric TTAGGG repeats alone is not sufficient to inhibit chromosome fusions, and that chromatin structure and telosome capping are essential for maintaining telomere integrity and protection[139,153,172,329].

6.4.3.2 Do shortened telomeres have increased fusigenic potential?

As discussed above, when folate is limiting, the frequency of uracil in DNA is increased. The subsequent repair response elicited by the cell significantly increases the likelihood of a SSB or DSB[74,75,92,100,365]. The rapid telomere shortening observed in WIL2-NS cells cultured in low FA medium from days 14-42 of the long term FA study (Chapter 4), suggests that breakage may be occurring. It was plausible that uracil incorporation, and subsequent DS breakage, may have resulted in the accelerated telomere shortening observed. Furthermore, clear evidence exists in the literature demonstrating a positive association between short telomeres, increased fusigenic potential, increased frequency of NPBs, and increased chromosomal chaos arising from BFB cycling[27,33,125,278,279,283,330,373]. As such, the findings of increased frequency and total number of NPBs in the FA study, in parallel with telomere shortening, is consistent with previous reports.

The findings of extremely high numbers of NPBs in the cells cultured in the presence of DNMT inhibitor, 5azadC, is not consistent with the uracil incorporation and telomere shortening model. Quite the reverse, in fact, with findings from this experiment showing that elongated telomeres correlate positively with NPB frequency. In addition, the cells cultured in 1.0µM 5azadC showed the highest frequency of BN cells with 'chewing-gum' morphology. While uracil incorporation into DNA is not a feature of 5azadC treatment, and telomere shortening was not observed, 5azadC has been reported to increase DNA damage, including sister chromatid exchange (SCE), gene amplification and chromosome rearrangements[356]. 5azadC has also been reported to cause increases in single and double strand breakage[356], and as such, may cause TL shortening in the longer term. It is therefore not implausible that

5azadC treatment might cause a small number of TL shortening events that may contribute to NPB formation.

6.4.3.3 Hypomethylation leads to recombination and potential BFB cycling

Subtelomeric hypomethylation arising from (i) reduced availability of methyl groups via S-adenosyl methionine (SAM) (*eg.* under folate limiting conditions), or (ii) direct inhibition of DNMT enzyme activity, may result in increased homologous recombination (HR) and increased sister chromatid exchanges involving telomeres (T-SCE)[319]. In turn, these mechanisms may result in (fusigenic) uncapped chromosome ends, dicentric chromosome formation, NPBs/BFB cycling and rapid changes in telomere content in cells (Figure 6.10).

The mammalian telomere sequence lacks CpG dinucleotides, the substrate required for cytosine methylation by DNMT enzymes, and as such are methylated only at histones[148,319]. The subtelomere, on the other hand, is heavily methylated both at histones and at cytosines within the DNA sequence[148,319,328]. It has been speculated that these epigenetic modifications may play a role in inhibiting HR, a feature observed in regions rich in repeating sequences[148,319]. Global methylation of cytosines, including at heterochromatic structures such as the pericentromeric region and the subtelomere, is effected by DNMT enzymes[319,328]. Features of mouse models genetically deficient for DNMT1 or DNMT3a & 3b included reduced subtelomeric methylation and elongated telomeres, while methylation at histones remained unaffected, indicating these markers are effected through different pathways[328]. It is also relevant to note that telomerase activity and levels of TRF1/TRF2 binding at telomeric chromatin were similar in DNMT-deficient mice, compared to WT controls[328].

The findings of the present experiments are consistent with those reported by Gonzalo *et al* (2006) (in a DNMT deficient mouse model) and Vera *et al* (200) (using a panel of human cancer cell lines)[319,328]. These studies provided strong evidence that hypomethylation at the subtelomere results in significant telomere elongation as well as enhanced recombination, as evidenced by increased T-SCE[319,328]. The direct mechanistic connection between hypomethylation and T-SCE was demonstrated, in the mouse model, by a partial restoration of methylation status, resulting in a reduction in T-SCE frequency[328]. The authors note that this partial restoration of methylation was not, however, sufficient to "reset" telomeres to a normal length[328]. This is interesting in the context of the present studies, in that the degree of hypomethylation observed from FA insufficiency was significantly less than that in the 5azadC-treated cells, while both resulted in significant, rapid increases in telomere content. Further exploration is required to determine the level of hypomethylation at which telomere

length and integrity is affected. It would also be interesting to determine, if possible, the level of folate required *in vivo* to maintain methylation for optimal telomere integrity. These concepts are consistent with observations in cells from ICF patients with a defective DNMT enzyme, in which hypomethylation was associated with random telomeric associations and NPBs[347].

It is proposed that increased levels of T-SCE may be instigating factors for end fusions leading to the formation of dicentric chromosomes and the high number of NPBs observed in WIL2-NS cells treated under hypomethylating conditions. In addition, T-SCE has been reported as a feature of ALT+ (neoplastic) cells which use HR as a means of maintaining telomere length[199]. Other features of ALT include highly heterogeneous TL, and ALT-associated promyelocytic leukemia bodies (APBs) where telomeres have been shown to co-localise with recombination-associated proteins[199]. TL heterogeneity and significant increases in APBs, compared with WT controls, were also observed in the DNMT-deficient mouse cells, suggesting that ALT is activated by hypomethylation of the subtelomere[328]. While the mechanism underlying this is not yet fully understood, it is proposed that methylation may repress the HR machinery[319,328]. Accordingly, it may be possible that the ALT mechanism is activated in the WIL2-NS cells under hypomethylating conditions, thus explaining the rapid increase in TL and the high frequency of NPBs, possibly arising from HR and T-SCE. Further studies should explore whether APBs are present, as well as the effects of methylation status on TL heterogeneity.

In summary of this section, it is proposed that the high number of NPBs observed in WIL2-NS cells under hypomethylating conditions are most likely attributable to a derepression of HR mechanisms, resulting in T-SCE, uncapped (fusigenic) chromosomes forming dicentric chromosomes and NPBs, leading ultimately to BFB cycling.

6.4.3.4 Could disruption of the cohesin pathway at telomeres lead to multiple NPBs and BN cells with 'chewing-gum' morphology?

An interesting study published by Dynek & Smith in 2004 showed cells at anaphase in which the nuclei were unable to separate due to the formation of multiple 'proteinaceous' bridges between telomeres[322]. This work demonstrated that knockdown of Tankyrase 1 (Tank1) inhibited release of telomere-specific cohesin proteins[322]. Cohesin complexes have been shown to hold sister chromatids together until the appropriate time in the cell cycle for separation[369]. The timely removal of cohesin complexes from chromosome arms at prophase by phosphorylation, and by proteolytic cleavage of a key subunit at centromeres at metaphase

is well understood[369]. The work of Dynek and Smith, however, identified a third group of cohesins present at telomeres which required Tank1 proteins to be activated by phosphorylation before chromosomes were able to separate at anaphase[322]. A related, study by Yalon *et al* (2007), investigated the timing of sister chromatid resolution at human telomeric regions and found that telomeres were fully resolved by metaphase[374]. Studies comparing young cells with ageing cells, however, indicated that as older cells approached senescence, cohesion at telomeres persisted abnormally[374]. NPBs were observed in these cells, a high proportion of which contained telomere signals[374]. Where wider NPBs were recorded, multiple telomere signals were present, suggesting multiple end fusion events[374]. Given the elevated levels of damage and CIN observed in ageing cells with shortened telomeres, the authors proposed that the prolonged cohesion may be a mechanism whereby the cell is able to pause the cell cycle while damage repair is undertaken[374].

Further studies into the biochemistry of cohesion at telomeres have shown that a complex of TRF1 and TIN2 bind to the SA1 subunit of the cohesin Scc3 protein[369]. It is known that Tank1 is phosphorylated at metaphase and that this then poly-ADP-ribosylates (PARSylates) TRF1. PARsylation of TRF1 causes a conformational change leading to its dissociation from the telomere[369]. The authors of this work propose that sister chromatid separation at telomeres is effected by the release of the TRF1/TIN2/cohesin complex at anaphase, which is initiated by PARsylation of TRF1 by activated Tank1[369]. They propose that the timing of this mechanism may be regulated by TIN2[369].

Cells displaying 'chewing-gum' NPB morphology were much more frequent in the cells treated with 5azadC, however, the impact of this chemical on TRF1 binding (and associated capping proteins) is not known. It is possible that adducts in the telomere sequence formed by 5azadC may impair TRF1 binding, however, adduct formation should have been minimised at the concentrations used in this study. Given the formation of multiple NPBs observed in the Tank1 knockdown cells[322], and their documented association with the telomere, and telomere binding proteins[322,369], it was important to consider the hypothesis that NPBs observed in the present study may be attributable to a defect in this pathway. At this stage, however, there is no mechanistic evidence linking DNA hypomethylation with impaired PARsylation of TRF1, and thus release of the TRF1/TIN/cohesin complex at anaphase.

Figure 6.10 (following page)

Proposed model of telomere content amplification via the breakage-fusion-bridge (BFB) cycle. Compromised telomere ends fuse forming a dicentric chromosome. The latter breaks at a random site during anaphase at the following mitosis, resulting in daughter cells obtaining aberrant, uncapped chromosomes with altered gene and telomere dosages. Daughter cells inheriting the smaller fragments of the broken dicentric chromosome may be rendered non-viable by these changes, or the uncapped chromosome may be replicated resulting in further end fusions, further NPB formation, breakage and a repetition of the cycle. The latter may lead to amplification of telomere sequences in the daughter cell that inherits the larger fragment of the broken dicentric chromosome. The BFB cycle is known to occur in numerous cancer cell types, and is believed to be responsible for the high level of chromosome instability and gene amplification observed in these cells.

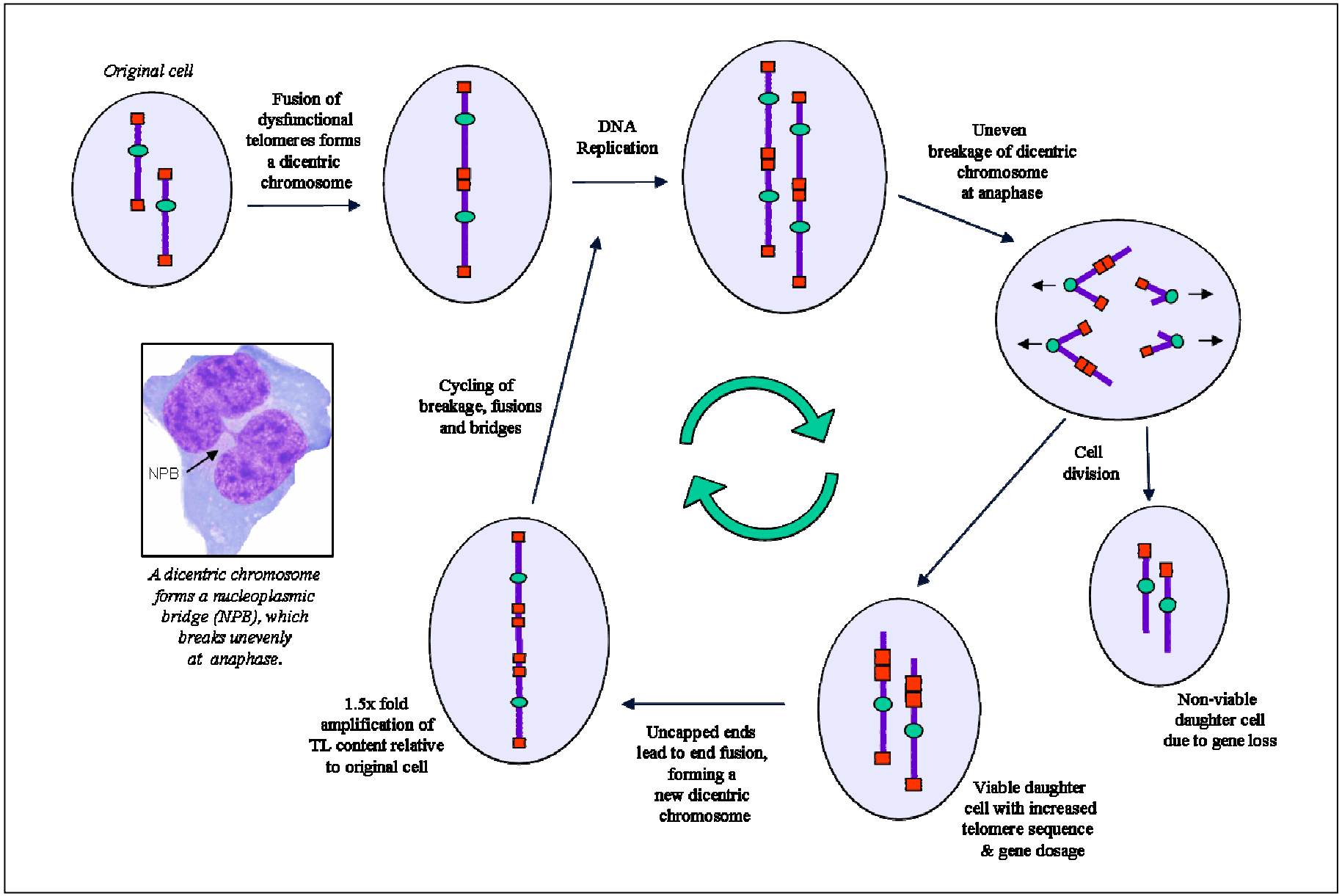
Original cell
Fusion of dysfunctional telomeres forms a dicentric chromosome
DNA Replication
Uneven breakage of dicentric chromosome at anaphase
Cell division
Non-viable daughter cell due to gene loss
Viable daughter cell with increased telomere sequence & gene dosage
Uncapped ends lead to end fusion, forming a new dicentric chromosome
1.5x fold amplification of TL content relative to original cell
Cycling of breakage, fusions and bridges
NPB
A dicentric chromosome forms a nucleoplasmic bridge (NPB), which breaks unevenly at anaphase.

6.5 CONCLUSIONS

- From these findings, it was concluded that FA insufficiency resulted in increased DNA hypomethylation and possibly increased uracil in telomeric DNA. These events occurred together with a greater frequency of BN WIL2-NS with multiple NPBs, compared to cells cultured in FA replete medium. Telomere length was positively associated with hypomethylation and NPBs. These results were in agreement with the hypotheses.

- It was also shown that WIL2-NS cells cultured in medium containing 0.2 or 1.0μM 5azadC have increased levels of DNA hypomethylation and an increased frequency of BN cells containing multiple NPB compared to cells cultured in 0uM 5azadC. Uracil content in telomeric DNA remained unchanged by 5azadC treatment. These findings, also, supported the proposed hypotheses.

- In both FA deficiency and 5azadC treatment the frequency of BN cells containing multiple NPBs was found to be positively associated with global hypomethylation as predicted by the proposed hypotheses. These results suggest that hypomethylation, either by FA deficiency or 5azadC treatment, leads to increased telomere dysfunction and fusigenic potential.

6.6 FUTURE DIRECTIONS

- Both the FA depletion and 5azadC *in vitro* studies should be repeated using fresh lymphocytes to determine if similar effects are seen in non-transformed cells.

- The degree of correlation between LINE1 global methylation and subtelomeric methylation should be investigated further.

- Determine the location and intensity of telomeric signal in nucleoplasmic bridges using fluorescence in situ hybridisation (FISH). In addition, the structure and composition of telomeres at fusion points of NPBs should be investigated to define, directly, changes in telomere structure that cause end-fusions.

- Using FISH, the presence of APBs should be explored to determine if the ALT mechanism is present in untreated WIL2-NS cells, in WIL2-NS cells cultured in low FA conditions, and in the presence of 5azadC.

- Telomere capping by TRF1 and TRF2 should be examined under conditions of low FA and/or 5azadC treatment, and any changes in capping examined with respect to their affect on telomere length or functionality.

- γH2AX is a marker for DNA damage such as strand breakage, and an initiating factor for a DNA repair response. The presence of γH2AX at telomeres should be investigated to determine if low FA or 5azadC treatment cause an increase in γH2AX foci, and if so, how this impacts on telomere length and functionality.